



Assistive Wearable Robots for Lower Limb Impairments

Author:

Amanda Bernstein

Supervisor:

Prof. Benny Lo

Co-Supervisors:

Rejin J. Varghese, Jindong Liu

A thesis submitted in partial fulfillment of the requirements for the degree of MRes in Medical Robotics and Image Guided Intervention and for the Diploma of Imperial College

September 2018

HAMLYN CENTRE

DEPARTMENT OF SURGERY AND CANCER

Abstract

This project aims to present both a low-cost soft wearable robot for ankle plantar and dorsiflexion as well as a tabletop model for a standing wheelchair. Wearable robots have been considered a promising alternative to traditional devices for mobility assistance, which approximately 10% of people need [1]. As the demand for mobility assistance devices is growing, it is important to develop new low-cost devices that can provide active assistance for daily activities. The first research objective is to develop a wearable robotic ankle system that can provide active assistance for those with weakness in the ankle, specifically drop-foot. Force sensors are coupled with a custom designed shoe insole, motor, bowden cable, and inertial motor unit to form the active ankle device. The control concept of a proportional control system with input from a machine learning classifier is proposed to provide real time control of the device. This system will only engage during the heel-strike or toe-off phases of the gait cycle and will change the speed of winding the bowden cable in proportion to how fast the angle of the ankle is changing. The results demonstrate the potential of this device to be used for walking assistance by those with drop-foot, thus providing a low-cost and soft alternative to current rigid wearable robotic devices that address drop-foot. The second research objective is to develop the framework for a standing wheelchair device with a novel knee component to provide assistance during sit-to-stand. The initial design calculations for this framework accounted for the shift in center of mass during the motion as well as the amount of load the linear actuator had to support during sit-to-stand. This framework was scaled down into a tabletop model that could follow the typical trajectory of the body during sit-to-stand. The tabletop model can be used for simulations of the novel knee design in addition to other design concepts regarding the standing wheelchair. Prospectively, these two devices could be combined into a novel device that can assist with both walking and sit-to-stand. **Word Count: 12,264**

Acknowledgements

I would like to thank my project supervisors Prof. Benny Lo, and Dr. Jindong Liu for their guidance and support. I would also like to acknowledge Rejin Varghese for his guidance and help on this project. I would like to thank the other members of the Hamlyn Centre, especially Mohamed Essam and Daniel Freer, for helping and advising me on several occasions. I would like to extend a very special thank you to Dr. Daniel Elson for coordinating the MRes program. Thank you to my fellow MRes students for their advice and encouragement throughout this project. Finally I would like to thank my family and friends for their endless supply of encouragement and motivation.

Contents

1	Introduction	7
2	Literature Review- Lower Limb Exoskeletons	11
2.1	Gait rehabilitation	12
2.2	Locomotion Assistance	13
2.3	Concluding Remarks	16
3	Ankle Device	17
3.1	Introduction	17
3.1.1	Literature Review	19
3.1.2	Biomechanics	20
3.2	Methods	23
3.2.1	System Architecture	23
3.2.2	Electronics and Processing	23
3.2.3	Experiment	25
3.2.4	Control	25
3.3	Results	34
3.4	Discussion	40
4	Wheelchair and Knee Framework	42
4.1	Introduction	42
4.1.1	Literature Review	44
4.1.2	Biomechanics	46
4.2	Methods	48

4.2.1	Center of Mass Calculations	48
4.2.2	Component Selection	50
4.2.3	Scaled Down Model	54
4.3	Discussion	56
5	Conclusions	59

List of Figures

1.1 Examples of end-effector robots	9
2.1 Examples of exoskeletons used for locomotion assistance	15
3.1 Sample of force sensor readings collected across one step in each of the four gait stages as shown on the figures above the force sensor reading.	21
3.2 System architecture of the proposed ankle device	24
3.3 Pseudo code of the initial control system	26
3.4 Pseudo code of the Proportional Controller (P-Controller) system	32
3.5 Overall control loop of the ankle device	33
3.6 Calibration curve of the force sensors used in the ankle device	34
3.7 Gait cycle based on force sensor data	35
3.8 The actual weight distribution measured (as a bar chart) from the toe and heel sensors and the corresponding normal distributions captured at the toe-off and heel-strike events of the gait cycles	36
3.9 Machine learning classifications for the four stages of the gait cycle based on input from the two force sensors	37
3.10 Training vs. testing accuracy with varying number of k neighbors	37
3.11 Confusion matrices of 6 of the tested machine learning classifiers	38
3.12 Change in angle of the ankle during 30 seconds of walking	38
4.1 Example of a standing wheelchair [91]	43
4.2 Sit-to-stand motion	46
4.3 The approximate locations of the center of mass of each of the segments of interest	49

4.4	Free body diagram for determining the length of the back wheel for a 15 degree ramp	50
4.5	Change in center of mass during sit-to-stand	51
4.6	Free body diagram of the wheelchair frame used to calculate the force on the linear actuator	52
4.7	Optimization of the linear actuator placement	54
4.8	Tabletop model of the wheelchair frame	55

List of Tables

2.1	Current Lower Limb Exoskeleton Devices	11
4.1	Current Standing Wheelchairs	43
4.2	Current Sit-to-stand Assistive Devices	44

Abbreviations

ADLs Activities of Daily Living

AFOs Ankle Foot Orthoses

COM Center of Mass

DoFs Degree(s) of Freedom

EDL Extensor Digitorum Longus

EHL Extensor Hallucis Longus

FSRs Force Sensitive Resistors

HAL Hybrid Assistive Limb

IMU Inertial Measurement Unit

KNN K-Nearest Neighbors

LEAD Light-weight Lower Extremity Assistive Device

P-Controller Proportional Controller

PID Proportional, Integral, Derivative

SCI Spinal Cord Injury

SVC Support Vector Classifier

SVM Support Vector Machine

Chapter 1

Introduction

Approximately 10% of all people in the United States require mobility assistance, and about 20% of people over the age of 65 need mobility assistance [1, 2]. The need for mobility assistance increases with age, but age is not the only factor. A person's mobility deterioration can also be due to stroke, spinal cord injury, or neuromuscular disorders affecting the lower limbs [2, 3, 4, 5, 6]. Stroke can leave the body with varying degrees of motor disability in both the upper and lower limbs and is the leading cause of long-term disability in developed countries [7, 8, 9, 10]. Gait and balance deficits after a stroke limit functional mobility and contribute to more than 70% of stroke survivors having a fall within 6 months [11, 12]. In regard to walking, hemiparesis in the lower extremity can also lead to reduced walking speed, endurance and step length [4, 12]. Furthermore, hemiparesis can result in impaired swing initiation and increased ankle plantarflexion at toe-off and limited ability to stand up from a seated position [4, 12]. However, with physical therapy and rehabilitation, it is possible to regain some motor function. The main goal of rehabilitation for stroke survivors is to help them regain the ability to independently complete Activities of Daily Living (ADLs) such as bathing, eating, and standing [13, 14]. These rehabilitation techniques are not only limited to stroke survivors; the elderly, those with spinal cord injury or neuromuscular disorders, and the chronically ill can benefit as well [15].

Rehabilitation is one of the most important phases of recovery for many stroke survivors, and should include physical therapy that is directed at specific training of skills and functional training [16, 17]. Traditional physical therapy relies heavily on the therapist's experience and

standardized subjective evaluations [7]. Therapy is usually focused on intense task-oriented repetitive training and emphasizes sit-to-stand training for those with lower limb impairments [7, 18]. The number of repetitions a patient completes during a therapy session corresponds to the effectiveness of the training, which is evidenced by an increased range of motion and alleviation of spasticity [18, 19]. However, during traditional physical therapy sessions, only about 85 repetitions are accomplished, which is very labor intensive for the therapist and costly for the patient [9, 19, 20]. Robotics has recently been used to augment traditional physical therapy by providing patients with more repetitions and leveraging therapists' time. This has resulted in cost effective extensions of therapy programs, new measures of impairment, and new therapy protocols [21].

Rehabilitation robotics can not only introduce new efficiencies into certain routine therapy activities, but also provide valuable objective data to assist in patient diagnosis, customization of therapy, adaptation of robotic control during therapy, assurance of patient compliance with treatment regimens, and maintenance of patient records. [9, 22]. There is a need and opportunity to use technology such as robotics to assist recovery, shifting rehabilitation mentality. The field of rehabilitation robotics moves beyond assistive technology; it helps an individual cope with the environment via physically interactive, user-friendly robots that facilitate recovery [22]. The goal of rehabilitation robotics is to help people recover the ability to complete ADLs or to potentially take over functionality as needed. The robots typically used in a rehabilitation setting are end-effector based robots, meaning they are grounded and only contact the user at the most distal part of the limb while indirectly influencing more proximal segments [19]. End-effector robots such as the MIT-MANUS, ACRE, CRAMER, NeReBot, MACARM, Lokomat, and Anklebot are typically used because they are simpler for therapists to handle, and easily adjust to fit different patients (Figure 1.1) [8, 23, 24]. However, end-effector robots

lack portability and specificity, and thus exoskeletons are a major point of interest for the next stages of robotic rehabilitation [23].



a) MIT-MANUS, b) Lokomat [25], c) NeReBot [26], d) Anklebot [27]

Figure 1.1: Examples of end-effector robots

Exoskeletons are mechanical structures that mirror the skeletal structure of the limb [24].

Unlike end-effector robots, exoskeleton based robots allow for independent and precise control of movement in a few limb joints [24]. They can be applied in a variety of ways including assistive rehabilitation, human power augmentation, impairment evaluation, resistance exercises, and haptic interaction in tele-operated and virtual environments [28]. Unlike the fixed-based robots previously discussed, exoskeletons offer better ranges of motion [22]. Rigid exoskele-

tons provide stiff mechanical support, allowing for the transmission of forces and torques without the user's limb experiencing any load [29, 30]. This is beneficial in rehabilitation because joints with low spasticity require increased force and torque to act upon the joint and can also be used to help with tremor suppression [29, 30]. In addition to filling the need for highly repetitive task movements in therapy, the portable nature of exoskeletons can also be used to take over functionality of the limb when necessary. There is a high demand for at-home rehabilitation devices for ADLs, such as standing up, in order to increase the frequency of training to result in better patient outcomes [31]. Exoskeletons are the ideal solution to this demand due to their portability [19, 24]. While exoskeletons have the potential to be widely beneficial especially for home use, there is still work to be done in making them lighter, portable, and easy to use (don and doff) [31].

The organization of this paper is briefly described here. Chapter 2 presents a literature review on lower limb exoskeleton systems that have been developed for rehabilitation, assistance, and human augmentation, focusing on those that affect both the knee and ankle. Chapter 3 will introduce a novel low-cost, soft assistive device for gait assistance targeted at the ankle joint, including the methods of developing the device, the control structure, and preliminary results of testing. The preliminary design of a transforming wheelchair, including initial results from a scaled-down model will be presented in Chapter 4. Finally, results will be summarized in Chapter 5, and future work will be discussed.

Chapter 2

Literature Review- Lower Limb Exoskeletons

This section discusses different developed and in-development exoskeleton devices based on their application and inputs, focusing on those that target the ankle and knee (2.1).

Table 2.1: Current Lower Limb Exoskeleton Devices

Device	Year	Country	Target joint(s)/ movement	DOF	Input	Control Strategy	Application
LokoMat [32]	2000	Switzerland	Hip F/E Knee FE	2	Force sensors	Predefined gait trajectory	Rehabilitation
LOPES [33]	2011	Netherlands	Hip F/E, Ab/Ad Knee F/E	3		Adaptive-oscillator based control	Rehabilitation
ReWalk [34]	2011	Israel	Hip F/E, Ab/Ad Knee F/E	3	Tilt sensor	Predefined gait trajectory	Assistive
Ekso [35]	2012	USA	Hip F/E, Ab/Ad Knee F/E Passive ankle joints	3		Predefined gait trajectory (and variable assists)	Assistive
BLEEX [36]	2005	USA	Active Hip F/E, Ab/Ad Knee F/E Ankle D/P Passive Hip I/E rotation Ankle I/E, Ab/Ad	7	Foot insole sensors Passive mechanical impedances	Sensitivity amplification	Augmentation
HAL [37]	2011	Japan	Hip F/E Knee F/E		EMG	Model-based control	Power Assist
NAEIES [38]	2009		Hip F/E, Ab/Ad Knee F/E Ankle D/P, Ab/Ad, I/E	6	Multi axis force/torque sensors	Sensitivity amplification	Augmentation
MINA [39]	2011	USA	Hip F/E Knee F/E	2	Pre- recorded joint trajectories	Predefined gait trajectory	Assistive
MindWalker [40]	2013	Netherlands	Active Hip F/E, Ab/Ad Knee F/E Passive Hip I/E rotation Ankle D/P	3 active 2 passive		Predefined gait trajectory	
BE [41]	2011	Italy	Hip F/E, Ab/Ad, I/E Knee F/E Ankle D/P, F/E	6	Force/ torque sensors	Model-based control	Power augmentation
eLegs [35]	2011	USA	Active Hip F/E Knee F/E Passive Ankle D/P	2 active 1 passive	Finite state machine	Predefined gait trajectory	Assistive
Tagliamonte et al. [42]	2013	Italy	Hip F/E Knee F/E	2	Adaptive oscillators	Adaptive-oscillator based control	Rehabilitation
MIT exoskeleton [43]	2006	USA	Hip F/E Knee F/E	2	Position and force/torque sensors	Predefined action based on gait pattern	Augmentation
H. He et al. [44]	2007	Japan	Active Hip F/E Knee F/E Passive Ankle D/P	2 active 1 passive	EMG	Fuzzy control	Assistive

The main applications for lower limb exoskeletons are gait rehabilitation, locomotion assistance, and power augmentation [20]. Gait rehabilitation focuses on helping patients with mobility disorders regain muscle strength and control [20]. Gait rehabilitation is necessary since neurological injuries can result in muscle weakness and impaired motor control, thus leaving people with slow, labored and uncoordinated limb movements and an asymmetrical gait pattern [34]. Gait rehabilitation is focused on provoking motor plasticity, allowing the patient to recover the ability to walk on their own [20]. Typically, exoskeletons used for gait rehabilitation focus on actively moving the hip and knee joints while keeping the ankle joints passive since the main function of human ankle joints is for body weight support [20]. Locomotion assistance is necessary to help those with little to no mobility of the lower limb complete necessary ADLs [20]. Exoskeletons are extremely beneficial in this particular application because they can provide external torques to move the necessary joints even when the user does not have enough power to initiate the motion themselves [20]. Exoskeletons and wearable robots used for locomotion assistance will be addressed in this section. Power augmentation can enable the user to perform a task they would not easily perform themselves [20]. However, power augmentation is typically utilized to enhance the abilities of healthy individuals. Therefore exoskeletons that are used for power augmentation will not be focused on in this paper.

2.1 Gait rehabilitation

Currently, exoskeletons used for gait rehabilitation are treadmill-based and provide body weight support. These devices are not portable, so are only used in rehabilitation facilities. One of these, the LokoMat, is commercially available. This device provides functional walking training for those with mobility dysfunctions [20]. It is a prime example of how robotic devices can not only address the limitations of manual physical therapy, but also lighten the

heavy workload on the physical therapist. The Lokomat is composed of three main systems, the robotic gait orthosis with 4 Degree(s) of Freedom (DoFs), a body weight support system, and a treadmill [20]. To achieve walking with maximum voluntary participation of the user, the Lokomat employs linear drives for actuation, force sensors to measure hip and knee joint torques, and an impedance controller to support the user as needed [20]. To further optimize the user's performance, the gait pattern is customized for each patient as well as the amount of guidance provided [45]. A similar device, the LOPES, also actuates the hip and knee from a treadmill mounted exoskeleton with the goal to evaluate motor skills and assist patients with walking rehabilitation [45, 46].

2.2 Locomotion Assistance

Many of the exoskeletons researched for locomotion are commercially available and use predefined gait trajectory as a control strategy. One such device, the ReWalk is available for both personal use, and use in a rehabilitation clinic (Figure 2.1). The ReWalk is a powered exoskeleton with crutches designed to help those with complete Spinal Cord Injury (SCI) walk independently using powered hip and knee joints [12, 46]. It is controlled by on-board computers and motion sensors, which sense the forward tilt of the upper body to initiate stepping [12, 20]. After the initial step, the device responds to subtle trunk motion and change in center of gravity to follow the pre-programmed sequence of steps [34]. However, the ReWalk is only available for patients who meet certain height and weight criteria [12].

The Ekso is another commercially available device to help those with limited mobility regain locomotion ability in daily life (Figure 2.1) [46, 47]. It has three DoFs per leg, controlling hip abduction/adduction, hip flexion/extension, and knee flexion/extension as well as passive ankle joints [20]. The Ekso is only for use in rehabilitation and has a variable assist feature to

allow the therapist to adjust the assistance level in each leg based on the user's need [20]. Like the ReWalk, the Ekso has a backpack to house the batteries and on-board computers in addition to the remote control [34]. While there are height and weight restrictions to using the Ekso, the frames are all adjustable to allow a comfortable customizable fit for each patient [45]. The Ekso also can work with a cane, walker, or crutches accessories to provide even more customization to the user.

A heavier and bulkier exoskeleton, the REX is commercially available for both home and clinical use (Figure 2.1) [34, 47]. Even though it is bulkier it can move into different static and dynamic stances, including squatting, so therapists can do various training exercises with the user [48]. It does not require external crutches for use to allow hands-free operation of the exoskeleton through the joystick controller [12]. Similar to the Ekso, only the hips and knees are actuated [48]. Even the most popular personal use exoskeleton, the Indego, only has actuated hips and knees [34]. Unlike the rest of the exoskeletons, it has a modular design, allowing the system to be disassembled and then reassembled when needed [49]. Another unique feature is the lack of a heavy backpack to house the battery and on-board computer. Embedded sensors throughout the exoskeleton estimate the user's intended movements based on changes in center of gravity and send the data to a mobile application, thus allowing wireless control [34].

The leader in the field of lower limb exoskeletons for locomotion assistance is the Hybrid Assistive Limb (HAL) developed by Cyberdyne (Figure 2.1). Some versions are commercially available, and most models are available only in Japan where the device was developed [12, 47, 50]. It uses an extensive number of sensors including myoelectric sensors and force sensors to detect both the exosuit position and the user's intention [51]. It was primarily developed to provide additional power to those with muscle weakness when walking or stair-climbing [46].

Consistent with most lower limb exoskeletons, only the hip and knees are actuated while the ankle is kept passive [46, 52]. However, unlike most commercial lower limb exoskeletons, the HAL uses bioelectric signals to estimate the user's intention and provide assistance as needed [34]. While the ability to estimate user intention makes HAL the leader in the field, it can take up to two months to calibrate the device to the specific user [52]. Unfortunately, all of these exoskeletons are expensive, and are not always covered by insurance.



a) ReWalk [53], b) HAL [54], c) Ekso [55], d) REX [48]

Figure 2.1: Examples of exoskeletons used for locomotion assistance

Some lower limb exoskeletons not commercially available are the MINA and eLegs. The MINA, developed by the Institute for Human and Machine Cognition, has three actuated DoFs on the hip and knees as well as two passive DoFs on the hip and ankle [46]. It is composed of a rigid frame with compliant actuation, which allows for variable impedance at the joints [34, 56]. The joints also contain sensors to track the desired motion for duplication [34]. Similar to

previous exoskeletons, it requires crutches for balance [34]. The eLegs, developed by Berkeley Robotics and Human Engineering Laboratory, also only has active hip and knee joints with a passively actuated ankle joint [46]. However, the passive ankles on this device are spring loaded in order to reduce toe drop [12]. Even with this, it requires the use of crutches for balance [12]. The device is equipped with pressure sensors under the soles, potentiometers, accelerometers, and gyroscopes to provide feedback to the system [12].

2.3 Concluding Remarks

While there are commercially available devices for lower limb rehabilitation as well as ongoing research and development of new devices, there is still room and a need for improvement. For example, one need requiring attention is the active control of the ankle. Most current systems passively control the ankle, which is good for locomotion assistance. However, without active control of the ankle, the muscle can atrophy due to nonuse. Therefore it is important to develop a device with active ankle assistance to promote the movement of the ankle while walking. A device that actively controls the ankle can also be useful for people with good leg control, but a weak ankle (i.e. drop-foot). This type of targeted device can be a less expensive alternative to a full lower limb exoskeleton device. The idea of targeting specific joints using wearable robots can be expanded to the knee for sit-to-stand tasks as well. Therefore, the aim of this paper is to address the current limitations in wearable robotics by presenting a novel low-cost soft assistive device for ankle dorsi- and plantarflexion as well as the preliminary designs for a standing wheelchair with a novel knee joint.

Chapter 3

Ankle Device

3.1 Introduction

Drop-foot, also known as foot drop, is a common affliction that frequently occurs due to injury to the peroneal nerve [13, 57]. It is the inability to lift the front of the foot caused by muscle weakness in the dorsiflexor as well as spasticity in the plantarflexor [11, 57, 58]. The peroneal nerve can be harmed by prolonged kneeling, frequent crossing of the legs, and knee or hip replacement surgeries [57, 59]. Drop-foot can also occur after trauma to the brain or spinal cord [57]. The muscles most affected by drop-foot are the tibialis anterior, the Extensor Hallucis Longus (EHL), and the Extensor Digitorum Longus (EDL), which help to clear the foot during swing phase of the gait cycle [59]. This impairment can lead to inadequate initial propulsion, insufficient foot clearance, and poor shock absorption at heel-strike [14]. Common treatments of drop-foot include rehabilitation, the use of ankle braces, and surgical operations [59]. Depending on the underlying cause of the drop-foot, a partial to full recovery is possible, usually within three months [59]. However, if the drop-foot is caused by a stroke or other neurological disorder, it could become a lifelong disability that needs continuous treatment [57]. In this case, ankle braces are usually worn to support walking to reduce the risk of falling.

Stroke is the leading cause of long-term disability in developed countries [15]. It can leave the body with varying degrees of motor disability in both the upper and lower limbs [7, 8, 9]. Gait and balance deficits after stroke limit functional mobility and contribute to more than 70% of stroke survivors having a fall within 6 months [10, 11]. Hemiparesis in the

lower extremity can also lead to reduced walking speed, endurance and step length, as well as impaired swing initiation and increased ankle plantarflexion at toe-off [12]. However, with physical therapy and rehabilitation, it is possible to regain some motor function and strengthen the flexor muscles. The main goal of rehabilitation for stroke survivors is to help them regain the ability to independently carry out ADLs such as bathing, eating, standing, and walking [7, 46].

Rehabilitation is one of the most important phases of recovery for stroke survivors, and should include physical therapy that is directed at the specific training of motor skills as well as functional training [16, 17]. Lower limb rehabilitation typically focuses on walking with body weight support and is very time consuming and expensive [12]. However, rehabilitation often leads to long-term benefits, so intelligent assistive devices could fulfill the need for long term rehabilitation and provide support for ADLs. When focusing specifically on drop-foot, Ankle Foot Orthoses (AFOs) are typically used. Currently commercially available AFOs are not active assistive technologies, they simply keep the ankle joint angle close to 90 degrees, preventing the foot from unnecessarily hitting the ground while walking [29, 60]. However, AFOs only prevent drop-foot from occurring; they cannot assist with foot-slap at foot down, which needs to be addressed in stroke survivors [61]. While the most commonly used method to treat drop-foot, they reinforce a pattern of nonuse by restricting joint position and movement [10, 14, 29]. The restricted use of the ankle joint can cause atrophy of the muscles, creating a long-term dependency on the device, leading to abnormal gait patterns [15, 29]. Due to these limitations, exoskeletons/exosuits are considered as an alternative to traditional AFOs.

3.1.1 Literature Review

Exoskeletons are mechanical structures that mirror the skeletal structure of the limb, allowing independent and precise control of a few limb joints [24]. They can be applied in a variety of ways including assistive rehabilitation, human power augmentation, impairment evaluation, resistance exercises, and haptic interaction in tele-operated and virtual environments [28]. Assistive devices are the ideal solution to the increasing demand for at-home rehabilitation devices for ADLs due to their portability [19, 24]. When applied to the ankle, assistive devices can help address the problems associated with drop-foot without restricting the ankle joint movement.

Typically, exoskeletons or assistive devices that are used for gait rehabilitation focus on actively supporting hip and knee joint movements, while keeping the ankle joints passive, since the main function of human ankle joints is for body weight support [20]. Keeping the ankle joints passive is a mechanical design not just with whole-leg exoskeletons, but for exoskeletons that focus specifically on the ankle [62]. However, these rigid exoskeletons tend to be heavy, require extensive power, have a short battery life, and can restrict movement. Soft exoskeletons can address these issues, but no soft exoskeleton is currently available commercially. These passive ankle exoskeletons use resistive elements (usually springs) to store and release energy, to assist with walking [14, 63, 64]. Even though passive ankle exoskeletons can be beneficial, the addition of active elements could provide more adaptable assistance. Locomotion assistance is necessary to help those with little to no mobility of the lower limb to carry out ADLs [20].

Active exoskeletons are extremely beneficial in such applications because they can provide external torques to move the necessary joints even when the user lacks the muscle strength to initiate the motion themselves [20]. Many of the current active devices, such as those researched by Polinkovsky *et al.* or Seel *et al.*, use actuators to control the stiffness of the spring,

and some use functional electrical or neuromuscular stimulation (FES/ FNS) in addition to the actuator and spring [52, 62, 65]. Park *et al.* amongst others are researching other active exoskeletons that use pneumatic muscles aiming to mimic human muscles without restricting any natural DoFs [29, 62]. However, these require tethering to an air tank, which reduces the portability of the device. Pneumatic muscles also behave in a non-linear way, thus making the proportional control of them more difficult than for DC motors [19]. A common limitation with current AFOs and exoskeletons is that they are not adaptable to variable walking speeds and often overlook the dynamics of walking in their design [66]. It is crucial to address this problem because walking speed increases or variation of gait could increase the likelihood of foot slap [66]. Current AFOs and exoskeletons are not able to raise the foot fast enough when the walking speed changes, nor able to cope with the variations in gait (such as sharp turns, varying paces, etc.) An active exoskeleton could adapt to varying gait patterns addressing the user's needs.

3.1.2 Biomechanics

The individual's biomechanical and physical characteristics have to be considered when designing an exoskeleton for the ankle in order to assist the movement of the ankle joint as naturally as possible [67]. One main feature of the ankle that needs to be considered is the dissipative forces that are encountered while adapting to weight-bearing and ground-reaction forces [68]. The ankle has a large contact area that is stable under static load, and can support forces up to 4.5 - 5.5 times the body weight when moving [69]. The ankle is composed of three articulations, the tibiotalar, fibulotalar, and tibiofibular joints that allow for dorsiflexion and plantarflexion [68]. Statistically, on average the ankle has 35 degrees of motion for inversion, 25 degrees for eversion, 50 degrees for plantarflexion, and 20 degrees for dorsiflexion, which

shall all be taken into account when designing an exoskeleton [69]. During plantarflexion, the maximum moment about the ankle occurs, which on average is 130 Nm at about 50 degrees per second [70]. Due to these constraints, 100W of power is needed to directly drive the ankle joint, however during the swing phase the torque necessary to drive the joint decreases thus decreasing the necessary actuation power [62].

To adapt to normal gait variations and enable natural walking patterns, the timing of the gait cycle must be considered. The gait cycle for walking can be categorized into four phases, namely the stance phase, swing phase, heel-strike, and toe-off (as shown in Figure 3.1) [71]. In the stance phase, one leg is in contact with the ground, and in the swing phase, one leg is swinging freely [71]. Heel-strike is the instant when the swing leg contacts the ground, and toe-off is the instant the swing leg leaves the ground [71].

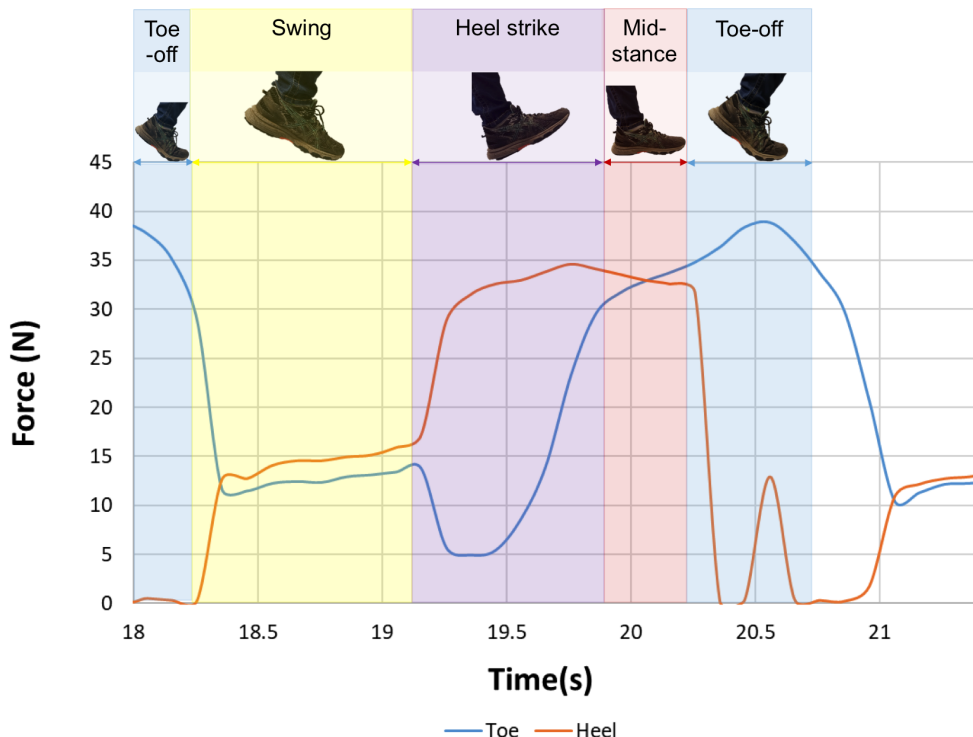


Figure 3.1: Sample of force sensor readings collected across one step in each of the four gait stages as shown on the figures above the force sensor reading.

If any point in the gait cycle is disrupted, the risk of tripping and falling increases. One common disruption to the gait cycle in people that have an impaired motor system is drop-foot [66]. This occurs during heel-strike when the foot falls uncontrollably to the ground (foot slap) and during toe swing when the toe drags, preventing proper limb movement and increasing the risk of tripping [66].

3.2 Methods

3.2.1 System Architecture

The proposed design is composed of two main elements:

1. The tendon-based actuation mechanism powered by a DC motor
2. A 3D printed insole connecting the tendon anchors to a shoe and housing the pressure sensors.

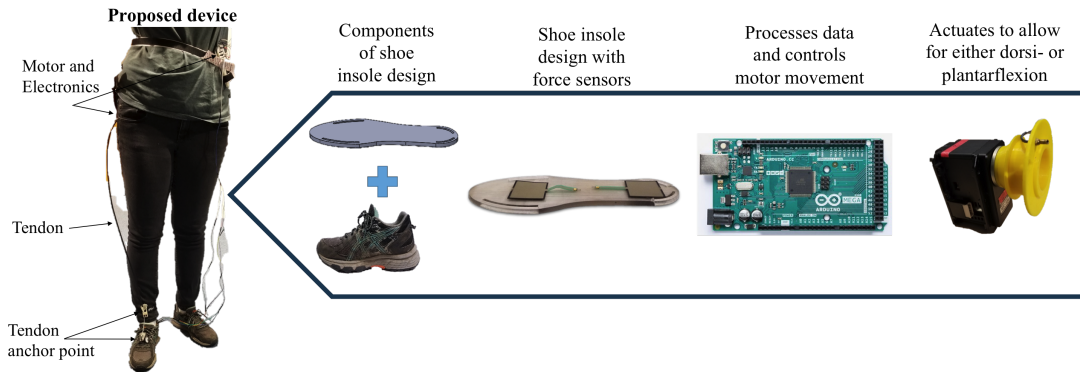
The Dynamixel Mx-106T (Robotis, California, United States) was used as the actuator.

A Bowden cable was anchored at the shoe laces by a 3D printed anchor piece connected to the printed shoe insole via Velcro straps. The cable ran across the top of the foot and up the shin where it was attached to the motor located on the back of the hip (as shown in Figure 3.2). The motor was transformed into a winch by attaching a custom designed and 3D printed drum to the end. The cable was secured to the winch drum so as the motor rotates, it either winds the cable up thus lifting the foot or provides slack to allow the foot to fall. The winch drum was printed in plastic using the Ultimaker 2 3D printer.

The Bowden cable was chosen in order to effectively route the tendon and offload the motor from the ankle, reducing the amount of weight on the target joint. A three-dimensional model of the insole was designed using SolidWorks, and was customized to fit the Gel-Venture 6 (Asics, Japan) trainer. This model was printed with plastic using the Fortus printer 450MC.

3.2.2 Electronics and Processing

The system utilized two FlexiForceTM A502 sensors (Tekscan, Massachusetts, United States) for measuring forces exerted by the foot on the ground during walking. The FlexiForce



(Left) The design of the proposed exoskeleton, and (Right) the components of the proposed exoskeleton. The 3D printed custom insole was combined with force sensors that were connected to an Arduino for data processing. The final proposed device combines all of the elements to form an assistive wearable robot for gait rehabilitation/assistance.

Figure 3.2: System architecture of the proposed ankle device

sensors are Force Sensitive Resistors (FSRs) that work on the principle of variable resistance with the application of variable force (i.e. the resistance across sensor terminals vary linearly as the force on the sensor varies). Before using these sensors for the system, calibration was required. This was achieved by stacking known weights (up to 3.1 kg) on the force sensor and recording the analog reading. A linear regression was used to find the linear correlation between the sensor readings and weights (3.1). Once the relationship between the analog reading of the force sensor and the corresponding amount of weight was calculated, the sensors did not have to be calibrated again.

$$y = 0.0963x + 0.22 \quad (3.1)$$

The proposed system uses the Arduino Mega (Arduino, Italy) as an embedded microcontroller, which samples the analog signal from the sensors and interfaces with the computing platform (laptop). These force sensors were attached to a custom designed shoe insole, one at the ball of the foot and one at the heel, so that gait parameters could be obtained in real-time (Figure 3.2). A custom shoe insole was designed rather than a leg brace, because it is lighter

and allows for a more natural range of movement. Unlike typical AFOs, the shoe insole design will not limit the inversion and eversion of the ankle, but will provide assistance in the dorsiflexion and plantarflexion ankle movements. In addition to the force sensors, a 9-axis Inertial Measurement Unit (IMU) was incorporated into the system. The IMU used was the MPU-9250 (Drotek Electronics, France), which has an accelerometer, gyroscope, and magnetometer as well as an on board digital motion processor. This was placed on the bottom of the insole, underneath where the arch of the foot would be. The motor was strapped to the back of the hip to distribute the weight and avoid impeding ankle movements (as shown in Figure 3.2).

3.2.3 Experiment

The analog output of each sensor was connected to the Arduino where it was sampled at 20Hz using its built-in 10-bit Analog to Digital Converter. The sampled data was transmitted to a laptop using UART protocol via serial to USB interface. As mentioned previously, two force sensors were used for measuring the foot movement during walking for data collection. Out of these 2 sensors, one was labelled as the heel, and the other labelled as the toe. To get baseline readings of the two force sensors, a subject walked for 30 seconds (repeated 20 times) (Figure 3.1). The 75kg subject was asked to walk at a slower pace to mimic the gait pattern of someone who suffers from drop-foot.

3.2.4 Control

Initial Control

From the baseline reading data, the maximum force of the heel during heel-strike and the toe during toe-off were recorded for each step. The baseline data was also used to determine the threshold ranges for detecting the heel-strike and toe-off events in order to initiate actuation

of the motor. The thresholds were manually determined by initially classifying the training data into four categories; heel-strike, mid-stance, toe-off, and swing.

The mean and standard deviation of the heel-strike and toe-off classes were calculated and shown as Gaussian distributions. From this data, the threshold of the heel and toe sensors for detecting both heel-strike and toe-off were determined. For both heel-strike and toe-off events, the information from the toe and heel sensors fell into two Gaussian distributions, with some overlap at the tails. The threshold was set at two standard deviations away from the mean in order to capture 95% the two distinct thresholds. This information was used to find the timing of an average step, which combined with the average force data to determine when to activate the, and how fast to pull the tendons. The motor control function is presented as the pseudo code (Figure 3.3).

Machine Learning

Initially, this system used manually set thresholds based on the normal distribution of the data to control the movement of the motor. However, it was imperative to create a more adaptable control system to refine the system for use in different settings. The first step in creating an adaptable control system was to implement real time machine learning classification to determine what stage of gait the user was in. Machine learning was implemented because typical gait analysis involves the description and assessment of features that characterize locomotion, which can be used in a machine learning algorithm to automate the process [72]. In this case,

```

1 function motor control (h ,t);
2   Input: Force on heel sensor h,
3     Force on toe sensor t,
4     Where, h >= 0 and t >= 0
5   Output: The motor control for two circumstances,
6     toe-off (to) and heel-strike (hs)
7   
$$f(h, t) = e^{-\frac{(h-\mu_h)^2}{2\sigma_h^2} + \frac{(t-\mu_t)^2}{2\sigma_t^2}}$$

8   initialize motor starting position;
9   if  $\mu_{to}^t - 2\sigma_{to}^t < t < \mu_{to}^t + 2\sigma_{to}^t$  and  $h < \mu_{to}^h + 2\sigma_{to}^h$  then
10    increment motor angle;
11    time delay;
12  else if  $t < \mu_{hs}^t - 2\sigma_{hs}^t$  and  $h < \mu_{hs}^h + 2\sigma_{hs}^h$  then
13    decrement motor angle;
14    time delay;
15  end
```

Figure 3.3: Pseudo code of the initial control system

supervised machine learning was implemented by training the classifier on the baseline data used to previously set the manual thresholds. Supervised machine learning was chosen since the goal was to classify the current stage of gait based on the baseline data. The force data from the toe and heel sensors were used as the input features, and the four stages of gait were labelled accordingly: 1 for heel-strike, 2 for midstance, 3 for toe-off, and 4 for swing. After the data was labelled, it was preprocessed to ensure there were no outliers or missing values. The data was then uploaded into a Jupyter notebook (Python) and split into a training and test set with 80% of the data being used for the training set. Once the data was split, the different machine learning classifications were tested to determine which would be the ideal one to use for the device. Seven machine learning classifiers were tested including Naive Bayes (Gaussian, Bernoulli, and Multinomial), K-Nearest Neighbors (KNN), Logistic Regression, Support Vector Machine (SVM), and Linear Support Vector Classifier (SVC).

Naive Bayes Gaussian

The Naive Bayes classifier is used in both binary and multi-class classification problems. This classifier is based on Bayes theorem, which is stated as 3.2:

$$P(h|d) = (P(d|h) * P(h)) / P(d) \quad (3.2)$$

where $P(h|d)$ is the probability of hypothesis h given the data d (posterior probability), $P(d|h)$ is the probability of data d given that the hypothesis h was true, $P(h)$ is the probability of hypothesis h being true (prior probability), and $P(d)$ is the probability of the data. Bayes theorem assumes that the presence of a feature in a class is not related to the presence of any other feature (conditionally independent). Due to this, the classifier is relatively fast, since no coefficients need to be fitted and only the different probabilities and conditional probabilities need

to be stored [73]. The class probabilities are the frequency of instances in each class divided by the total number of instances and the conditional probabilities are the frequency of each attribute for a given class divided by the frequency of instances with that attribute [73]. As new data is received, it is categorized based on the highest probability of it belonging to a particular class [74]. The Gaussian Naive Bayes Classifier is an extension of the Naive Bayes classifier that stores the means and standard deviations of each input variable for each class in addition to the probabilities. Then, the class of the new input is predicted using the Gaussian Probability Density Function [73]. This classifier assumes the data is normally distributed, which is why it was the first classifier tested on this data. Based on the results discussed in the next section, the Gaussian Naive Bayes classifier was the one chosen in the final control system of the device.

Bernoulli

The next classifier tested was a Bernoulli Naive Bayes classifier. The Bernoulli classifier is another extension of the Naive Bayes classification method. In this, the features are considered independent binary variables that describe the inputs. The model ignores the number of occurrences when using binary occurrence information, which makes it more prone to mistakes. It is also the only model that models the absence of terms explicitly [75]. However, Bernoulli classification works best for binary classifications, so even though it was tested, the results were expected to be poor.

Multinomial

Multinomial Naive Bayes was the next classification method tested. It works similarly to the Bernoulli Naive Bayes classifier, however it assumes that the distribution of the data is in a multinomial distribution as opposed to a Bernoulli distribution. Unlike the Bernoulli classifier, the Multinomial classifier counts the frequency of multiple features instead of the pres-

ence/absence of one feature. It is mostly used for text classification in documents or emails, so was not expected to perform as well as the Gaussian Naive Bayes classifier.

K-Nearest Neighbors

KNN is a common classification technique due to its easy to interpret output and fast calculation time. Unlike the Naive Bayes classifiers, it categorizes the features based on the classes of the majority of its nearest neighbors [74]. This method assumes that objects near each other are similar. Weights can be added to ensure that the nearest neighbors have the most impact on the average than the more distant ones. To determine the nearest neighbors, different distance metrics such as Euclidean, city block, cosine, and Chebychev are used [74]. KNN is one of the simpler classification methods because it does not explicitly require training. For this method, the number of neighbors (k) analyzed needs to manually be chosen. This is done by finding the point in which the training error rate and the validation error are optimized. It is important to find the best k value to use because if k is too low, the classification can be noisy and more vulnerable to outliers. If k is too high, the data can become smoothed over to the point where a category with only a few samples will always be outvoted by other categories.

Logistic Regression

Logistic regression is a statistical methods technique that is used in machine learning. It is usually used for binary classification, so the accuracy in classification from this method was not expected to be as good as from the Naive Bayes classifiers. This technique is based on the logistic or sigmoid function, which rises quickly and then maxes out. The logistic function is used to transform the probabilities into binary values in order to make a prediction [76]. Using this method, the input values are linearly combined using weights to predict the output. Unlike a linear regression, the output is a binary value instead of a numeric one [77]. Logistic

regression models the probability that the input belongs to the default class [77]. As shown in Equation 3.3, the model takes into account the bias (b_0) as well as the coefficient for each input value (b_1) [77].

$$y = e^{(b_0 + b_1 * x)} / (1 + e^{b_0 + b_1 * x}) \quad (3.3)$$

These coefficients are estimated from the training data by using maximum-likelihood estimation. Logistic regression is very efficient, easy to interpret, easy to implement, efficient to train, and is fairly accurate in predicting probabilities [76]. Due to this, it can be a good baseline to compare more complicated classification techniques to. However, it is not very powerful, and only works with linear data. While the most useful for binary data, it is possible to use logistic regression for multiclass classification.

Support Vector Machine

SVM is a classification method that classifies data by finding the linear decision boundary separating the data points in the classes. For linear data, the goal is to find the decision boundary so there is the largest margin between the classes. The margin should be equal distance away from each class. If the data cannot be separated linearly, a loss function is introduced to penalize points that fall on the wrong side of the boundary [74]. It is possible to use a kernel transform with SVM to change the nonlinearly separable data into a higher dimension where a linear boundary can be found [74].

Linear Support Vector Classifier

Linear SVC is used to find a best fit hyperplane that divides or categorizes the data [78]. It is similar to SVM, except it uses a one versus the rest approach for multiclass classification instead of a one versus one approach. The one versus the rest approach fits one binary classifier per

class, which provides the ability to learn about the class based on just the classifier information [79]. When classifying new data, the one versus the rest approach chooses the maximum value out of each of the probabilities from binary classifications [80]. It also uses a linear kernel for the basis function as opposed to the radial basis function (similar to a Gaussian kernel) that SVM uses.

P-Controller

In addition to the machine learning classification, a P-Controller was introduced to the system. This is the simplest part of a Proportional, Integral, Derivative (PID) control system. Even though it is not as complex as the full PID control system, it is more complex than the initial threshold system that was previously used. The P-Controller was used as a control loop feedback mechanism to close the system. This control mechanism applies a correction to the controlled variable, in this case the speed of the motor, that is proportional to the difference between the desired value and the measured one. The difference between the desired value and the measured one is the error of the system. This error is then multiplied by a proportional gain (K_p), which needs to be tuned so the system can perform optimally. While using just a P-Controller is simpler, it tends to increase the maximum overshoot of the system. It is also important to choose the right K_p value when only using a P-control system because too high of a K_p value can lead to the oscillation of the measured process variable [81].

In the proposed system, an IMU was introduced in order to implement the P-Controller. Using the IMU, the change in angle of the ankle throughout the movement could be recorded. The angle measurement was used in the P-Controller so the speed of the motor changed based on how fast the ankle angle was changing. The goal was for the motor to slow down as the ankle reached the target angle so that overstretching of the ankle would not occur. Due to

the fast sampling rate of the accelerometer on the IMU (10 Hz), the incoming readings had to be averaged. The average was taken of 10 incoming readings, so only angle per second was recorded. The difference between the current position and the average was then taken and converted to a hexadecimal value that the motor can interpret. This value was then multiplied by the K_p value, and a controller bias of 50 rotations per minute (rpm) was added on. The absolute value of this computation was used to control the speed of the motor while the position of the motor was controlled by the current angle reading from the IMU (Figure 3.4).

This whole process was initiated after toe-off or after heel-strike. After toe-off, the target position was 15 degrees for ankle dorsiflexion and after heel-strike, the target position was 0 degrees for ankle plantarflexion. In this way the Bowden cable will either lift the front of the foot into position for heel-strike, or lower it down for midstance while keeping tension on the cable throughout the motion.

The overall control loop uses the input from the force sensors to classify the stage of gait. Based on this classification the motor is initiated and the P-Controller is activated. Based on the feedback from the IMU, the system will

```

1 function motor_control (h ,t, a);
Input: Force on heel sensor h,
        Force on toe sensor t,
        Angle of foot, a
        Where, h >= 0 and t >= 0
Output: The motor control for two circumstances,
        toe-off (to) and heel-strike (hs)

2 initialize motor starting position;
3 if to then
    while (error > 0.5)
        error = abs(15 - New angle)
        average angle readings from IMU
        motor speed= abs[Kv * (current angle - average)]
        if no movement then
            move to goal position
        else
            increment motor angle at motor speed;
        end

4 else if hs then
    while (error > 0.5)
        error= abs(0 - New angle)
        average angle readings from IMU
        motor speed= abs[Kv * (current angle - average)]
        if no movement then
            move to goal position
        else
            increment motor angle at motor speed;
        end

```

Serial Event to read and classify stage of gait

Figure 3.4: Pseudo code of the P-Controller system

stop once the target position is reached. Once the target position is reached, the system waits until it receives the triggering gait classification (toe-off or heel-strike), and then repeats the loop (Figure 3.5).

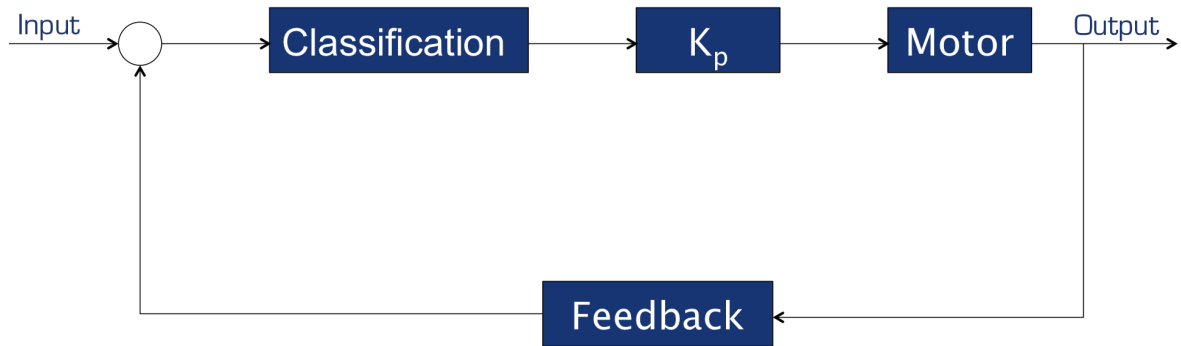


Figure 3.5: Overall control loop of the ankle device

3.3 Results

Due to the linear response of the force resistive sensors, a linear equation was determined and used as the calibration equation ($R^2 = 0.9958$) (as shown in Figure 3.6).

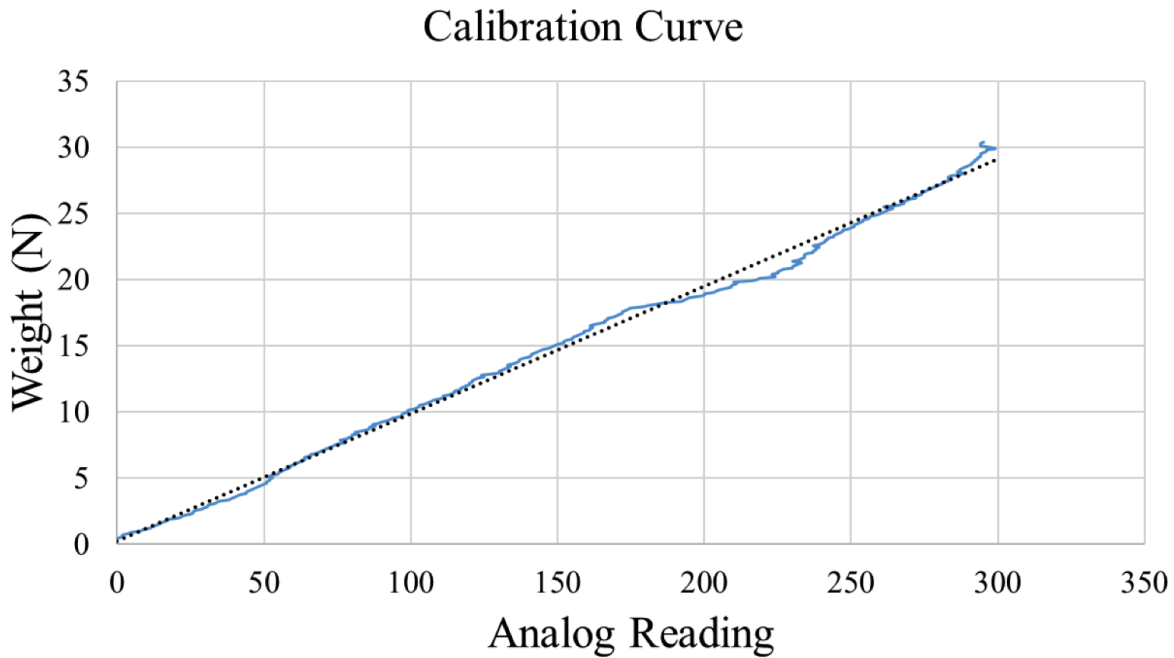
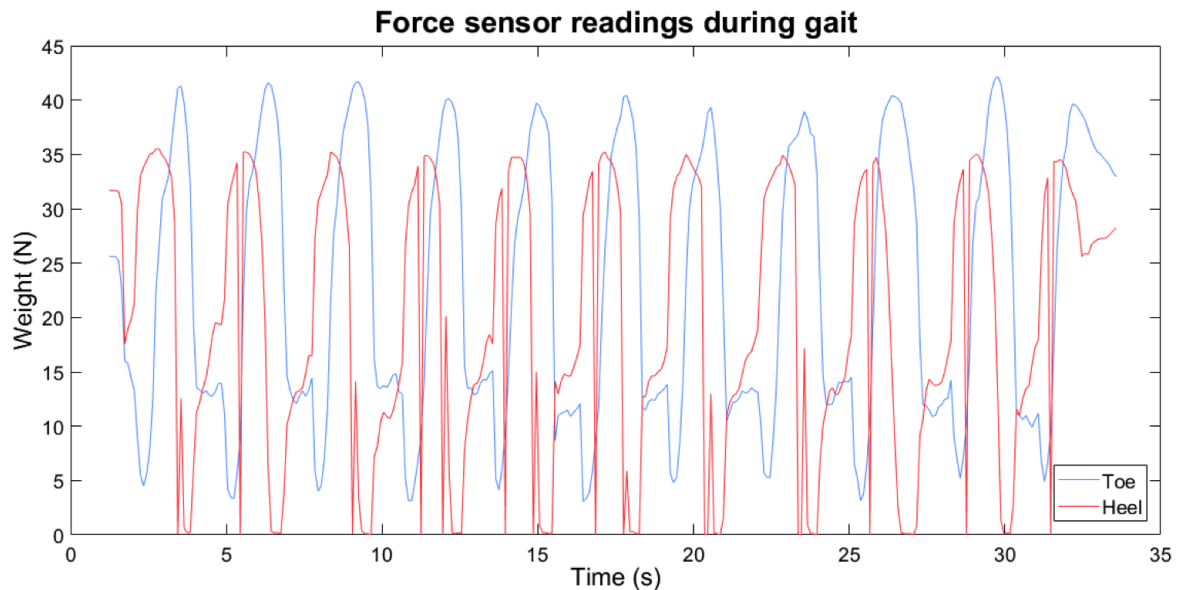


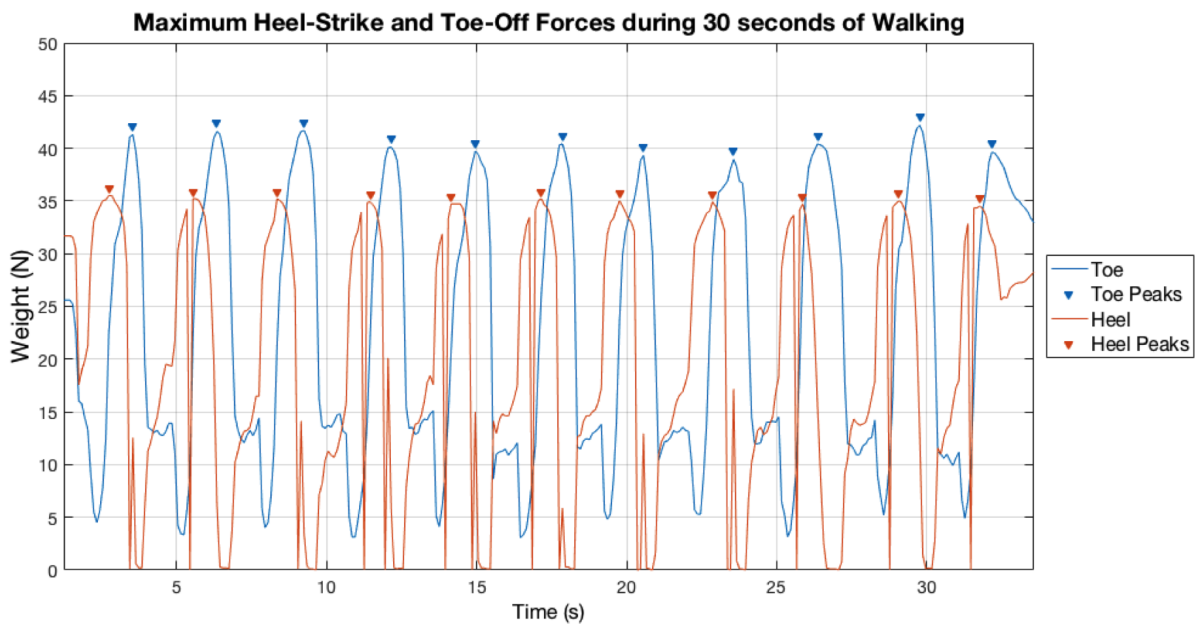
Figure 3.6: Calibration curve of the force sensors used in the ankle device

This equation was used to determine the heel-strike and toe-off forces for every step of twenty 30 seconds walking trials by converting the analog readings that were recorded into known weights in Newtons. The average maximum force for heel-strike and toe-off were found (31.54 N, 35.52 N, respectively) and used to determine the parameters for activating the motor. Analysis of only the two gait sensors produced a clear gait pattern as shown in Figure 3.7.

The difference between toe-off and heel-strike was then calculated to determine the period of the swing phase. On average the swing phase lasted approximately 1 second. This information was initially used to control a motor to actuate after toe-off and heel-strike, thus preventing foot drop or toe slap. As shown in Figure 3.8, Gaussian distributions were found for the heel and toe at both heel-strike and toe-off. During heel-strike, 2 distinct distributions were found (toe



(a) Force sensor readings showing the gait cycle



(b) Labelled peaks of force sensor readings to calculate period of swing phase

Figure 3.7: Gait cycle based on force sensor data

and heel) with the mean and standard deviation equal to $3.04 \text{ N} \pm 5.49 \text{ N}$ and $31.54 \text{ N} \pm 2.72 \text{ N}$ respectively. There were some outliers in the heel data that caused some overlap between the two classes. However, this overlap (at 20 N) occurs outside of two standard deviations for either class, so did not affect the control mechanism. Similarly, during toe-off, the two classes overlapped between 20 N and 25 N. This overlap was also outside of two standard deviations for either class, so did not affect the control mechanism. The means and standard deviations of the toe and heel during toe-off were $35.52 \text{ N} \pm 6.3 \text{ N}$, and $5.89 \text{ N} \pm 3.85 \text{ N}$ respectively.

Using the initial control system, after detecting toe-strike, the motor takes 0.8 seconds to complete a 20° rotation in the clockwise direction, lifting the toe upward into dorsiflexion, preparing the heel for heel-strike (Figure 3.3). Then, after heel-strike is detected, the motor takes 0.8 seconds to complete a 50° rotation in the counter-clockwise direction, preparing the toe for toe-off (Figure 3.3). The time was chosen as 0.8 seconds to ensure the foot is in the correct position before the gait event (toe-off or heel-strike) that on average occurs 1 after the previous one.

To develop a more advanced control system, a machine learning algorithm was introduced. The gaussian naive bayes, bernoulli, multinomial, KNN, logistic, SVM, and linear SVC were all tested to determine which was the most effective at classifying the four stages of gait. From just the force sensor data, the four distinct stages of gait could clearly be seen (Figure 3.9).

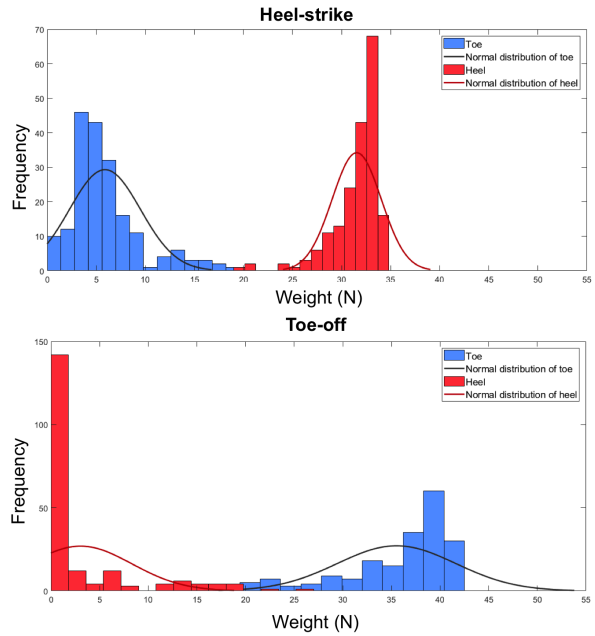


Figure 3.8: The actual weight distribution measured (as a bar chart) from the toe and heel sensors and the corresponding normal distributions captured at the toe-off and heel-strike events of the gait cycles

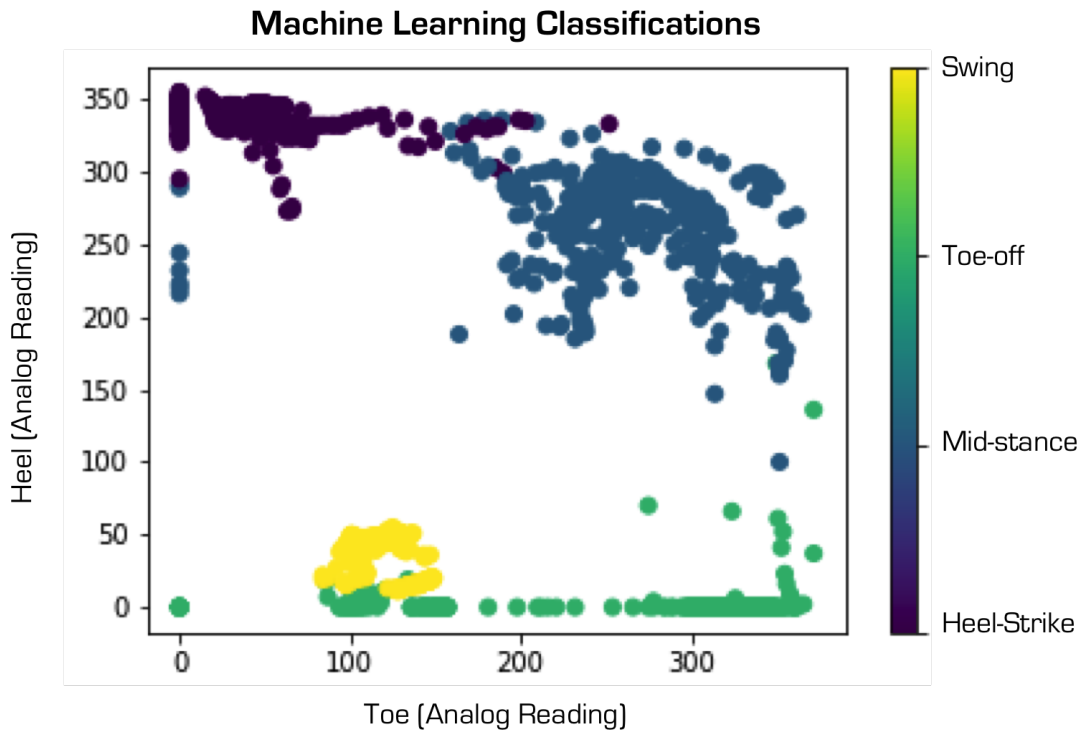


Figure 3.9: Machine learning classifications for the four stages of the gait cycle based on input from the two force sensors

To get the best result from the KNN classifier, the optimal number of neighbors (k) had

to first be determined. At 4 neighbors, the validation error and training error rate were optimized (Figure 3.10) and the accuracy was 98%. After the various machine learning al-

gorithms were tested, accuracy scores were calculated for each classifier to determine

which was the best to use (Figure 3.11). Confusion matrices were generated for the gaussian naive bayes, bernoulli, multinomial, logistic regression, SVM, and linear SVC classifiers and a confidence score was calculated for the logistic classifier (Figure 3.11).

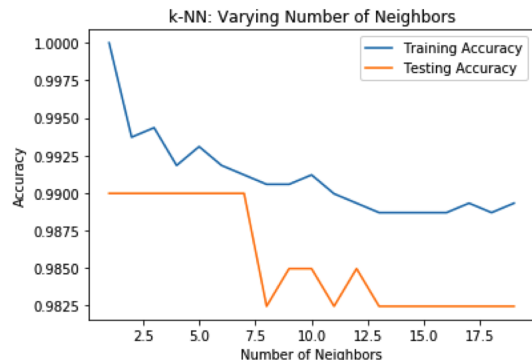
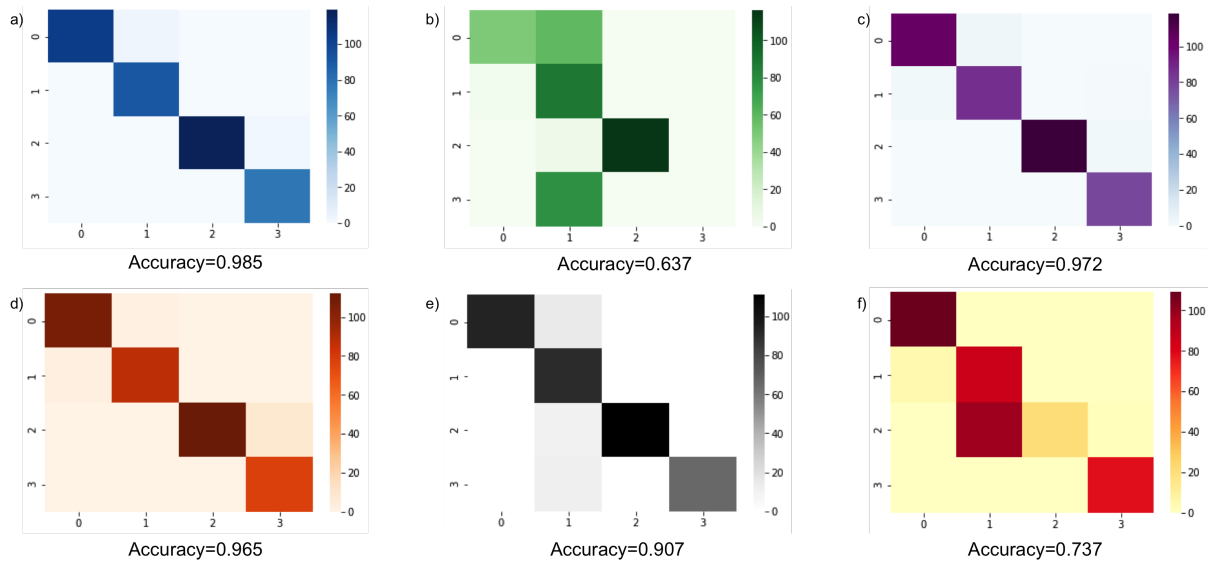


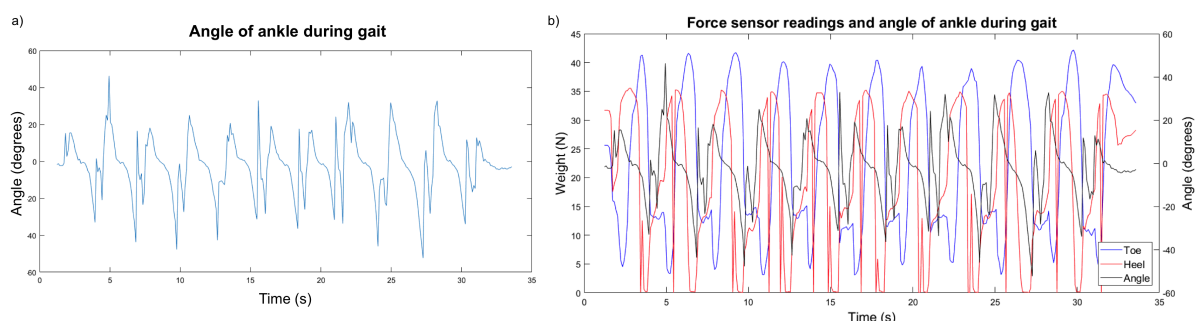
Figure 3.10: Training vs. testing accuracy with varying number of k neighbors



a) Confusion matrix and accuracy score for Gaussian Naive Bayes classifier, b) Confusion matrix and accuracy score for Bernoulli classifier, c) Confusion matrix and accuracy score for Multinomial classifier, d) Confusion matrix and accuracy score for Logistic Regression, e) Confusion matrix and accuracy score for SVM classifier, f) Confusion matrix and accuracy score for Linear SVC classifier

Figure 3.11: Confusion matrices of 6 of the tested machine learning classifiers

Based on these graphs, the gaussian naive bayes classifier was chosen for the system because it had the highest accuracy score (98%) and fit the data the best. To complete the more advanced control system, an IMU was added into the system architecture. After integration, the relationship between the change in angle of the ankle and the stage of gait was more clearly seen (Figure 3.12).



a) Example of IMU data collected during 30 seconds of walking
b) Combined IMU and force sensor data for 30 seconds of walking

Figure 3.12: Change in angle of the ankle during 30 seconds of walking

As expected, the angle changed from approximately -40 degrees (plantarflexion) to approximately 20 degrees (dorsiflexion). This coincided with the 50 degrees of plantarflexion and 20 degrees of dorsiflexion the ankle experiences during gait. Based on these measurements, the change in angle throughout the gait cycle was used in the P-Controller.

3.4 Discussion

This paper proposed a novel low-cost, soft assistive device for gait assistance for drop-foot. With our initial prototype, we have demonstrated the potential of the proposed device as a low-cost solution for providing assistance to stroke patients with drop-foot. The shoe insole design is lightweight, and does not restrict ankle movement, thus addressing the limitations of rigid exoskeletons/exosuits. However, this prototype needs further development before it can be deployed as a gait assistive device. A fully functional gait assistive device should be portable, lightweight, easy and comfortable to wear, and be adaptable to various gait patterns. The main limitation of the proposed device is the lack of portability. The device currently needs to be tethered to a computer for processing sensor data and an external power source for power. As a next step, a wireless microcontroller that utilizes Bluetooth could be used to enable wireless connection and eliminate the need for tethered wires, allowing for more portability. A wearable battery pack will also need to be added to the system for complete portability. The incorporated IMU can be used to obtain other gait parameters, such as walking speed, which can be used to train a more accurate and robust machine learning algorithm. This algorithm can be used as part of the control system, thus potentially improving the accuracy of the system. The data from the IMU can also be used to develop a PID control system instead of the current P-control system. This can make the device more adaptable to changes in speed, or can be used to make the system only assist as needed. The capability to assist as needed would be crucial for the device to be used as a rehabilitation tool and not just an assistive device. The methods presented could be used as a platform for a regression-based machine learning approach to identify real-time changes in gait speed to provide variable actuation speed with variable walking speed. The proposed low-cost assistive device is targeted for stroke survivors suffering from drop-foot,

addressing their long-term need for gait assistance, however it is not limited to that population. This device can also be extended to provide gait assistance for those recovering from peroneal nerve injury, and assist people with other neuromuscular disorders.

Chapter 4

Wheelchair and Knee Framework

4.1 Introduction

Sit-to-stand is one of the most complex and demanding activities performed daily, and typically is performed 60 times a day on average [82, 83, 84, 85]. It is considered one of the key factors in maintaining functional independence, however due to the increased physical demand on the body during this task, it becomes harder to perform with age [85, 86]. In the United States alone, there are about 50 million people over the age of 65, and 18% of them have limited mobility [2]. Approximately 2 million of this group have difficulty performing the sit-to-stand motion without external help [2]. With an aging population and labor shortage in the home health care industry, comes a need to develop assistive devices to help people maintain their functional independence for as long as possible [87].

The need for assistive devices extends not only to the elderly, but for those in wheelchairs as well. Wheelchair transfers are one of highest-scored essential mobility skills for daily life, and require completion of the sit-to-stand motion [88]. A wheelchair transfer is the process of moving from the wheelchair into bed, the toilet, or another chair. Nearly 2.2 million people in the United States rely on wheeled mobility devices in their daily life [89]. No matter the reason for needing a wheelchair, it has been found that sitting in a wheelchair for long periods of time can lead to a multitude of secondary health conditions [89, 90]. These can include reduction of bone mineral density, joint stiffness, muscle shrinkage, problems in blood circulation, pressure sores, back pain, and decreased respiratory function [89, 90]. To address these concerns, the

standing wheelchair was invented to help prevent some of these conditions.

Standing wheelchairs allow the user to move into an upright position, even if they do not have the ability to stand on their own (Figure 4.1). Many of these are commercially available, and are considered indispensable in the medical field due to their alleviation of the negative health effects caused by sitting as well as their potential for rehabilitation [38, 90]. They are also important in making the wheelchair user feel more included in their environment [92]. However, they can be expensive (£4,000 - 25,000) and most models cannot move while they are in the standing position (Table 4.1). There is currently work on developing manual wheelchairs to make them mobile while in a standing position, however none are currently commercially available [92].



Figure 4.1: Example of a standing wheelchair [91]

Table 4.1: Current Standing Wheelchairs

Device	Year	Country	Type of wheelchair	Manual or electric	Commercially available	Price
Eguchi <i>et al.</i> [6]	2013	Japan	Stand up		No	
LEVO AG [91]		Switzerland	Stand up	Either	Yes	£5,000-12,000
Superior		Sweden	Stand up	Manual	Yes	£7,500
Jive up [93]		Germany	Stand up	Electric	Yes	£17,000
Genie V2[94]	2014	UK	Stand up	Electric	Yes	£19,000
Karman[95]	1993	USA	Stand up	Manual	Yes	£6,500-13,000
Nickel <i>et al.</i> [92]	2016		Stand up	Manual	No	
iBOT[96]		USA	Rising	Electric	No	\$25,000
Elevation [97]		Canada	Rising	Manual	Yes	£4000
Manual Standing Wheelchair[98]		USA	Standing	Manual	No	
Up n' Go/ Up n' Free [99]		USA	Standing	Manual	Yes	£22,650-3,400
Laddroller [100]	2016	Greece	Standing	Electric	No	

4.1.1 Literature Review

A wearable robotic device could be used as an alternative to developing a fully mobile standing wheelchair. However, the sit-to-stand motion is more demanding for both the patient and the device [82]. Due to this, many of the devices created to assist those with limited mobility including sit-to-stand tasks are not wearable devices (4.2). They tend to take the form of a walker or chair that pushes the user up into a standing position. While these can help people stand, the user must be able to first move themselves into the seat of the device prior to the sit-to-stand motion. One such device developed by Furusawa *et al.*, is a chair equipped with two linear actuators, pantograph mechanisms and a switch. While it takes up less space than commercially available devices, it is stationary, so cannot assist throughout the day [101]. Similarly, Kamnik and Bajd developed a device that resembles half of a seesaw. The device is composed of a bike seat with force sensors and linear hydraulic actuators that raise the user into a standing position while they hold onto a frame [104]. This device showed potential for assistive or assessment purposes; however like Furusawa *et al.*'s device, it is stationary so it can only be used where it is installed. Other walker-like designs support the user's upper body and assist with completion of the sit-to-stand motion by pushing up on the arms instead of pushing from the seat. Both Kim *et al.* and Salah *et al.* have developed sit-to-stand assistive devices that

Table 4.2: Current Sit-to-stand Assistive Devices

Device	Year	Country	Target population	Input	Mechanism	Application
Furusawa <i>et al.</i> [101]	2017	Japan	Disabled	Switch	Push up	Assistive
Kim <i>et al.</i> [51]	2011	Korea	Elderly and disabled		Walker	Power Augmentation
Salah <i>et al.</i> [102]	2013	Egypt	Elderly	Inertial sensors	Walker	Assistive
Allouche <i>et al.</i> [83]	2017	France	Stroke		Push up	Assistive
Putra <i>et al.</i> [90]	2017	Indonesia	SCI	Push button and switch	Push up	Assistive
LEAD (Shen <i>et al.</i>)[103]	2013	Singapore	Stroke	EMG and force sensors	Actuators at joints	Assistive
Mefoud <i>et al.</i> [2]	2012	France	Disabled	Electrogoniometer		Assistive
Kamnik and Bajd [104]	2007	Slovenia	Disabled	Force/ torque sensor	Push up	
Chugo <i>et al.</i> [105]	2007	Japan	Elderly	Force/ torque sensor	Walker	Rehabilitatioon
HAL (Tsukahara <i>et al.</i>) [18]	2010	Japan	Paraplegic	Potentiometer, accelerometer, and force sensors	Actuators at joints	Assistive
Alter G [106]	2005	USA	Unilateral neurological or orthopedic conditions	Pressure sensors, accelerometers, and joint angle detectors		Rehabilitatioon
Vose <i>et al.</i> [84]	2013	USA	Stroke			Power Augmentation
Pott <i>et al.</i> [107]	2017	Germany	Elderly	Strain gauges and force sensors	Actuators	Power Augmentation

support and push the arms. These devices are beneficial in supporting the user's body weight as they walk, but they rely on the user having the capability to walk and support their own body weight [51, 102].

As an alternative to these typically stationary walker-like devices, wearable assistive robots are currently being developed. For example, Pott *et al.* have developed a knee-ankle-foot orthosis for the elderly using series elastic actuators, muscle activity sensors, and force plates mounted on a shoe to determine what type of support to the knee relieves biomechanical loads and thus reduces the muscular demand of the user performing sit-to-stand motions [107]. However, this device was heavy and consumed too much power. Shen *et al.* developed a Light-weight Lower Extremity Assistive Device (LEAD) to aid stroke patients during rehabilitation [103]. This device uses force sensors and EMG signals to inform the finite state machine controller of the user's intended motion. The current leader in the field, however, is the HAL which bears some similarities to the LEAD device. HAL is a robosuit that can infer the user's intention before they perform the desired motion in order to provide the optimal assistance. HAL was designed to support a variety of people (healthy to paraplegic) using bioelectric signals and force sensors [18]. While these devices have showed potential as assistive lower limb wearable robots, the LEAD is not commercially available and some versions of the HAL are only available in Japan.

Current devices that assist with completing the sit-to-stand motion fall into either the stationary or wearable robotics categories. While some, such as the HAL, are very advanced and can complete the movement based on the user's intention, none are versatile enough to function as a wheelchair that can also perform the sit-to-stand motion. Therefore, the aim of this research is to develop a simulation of a novel sit-to-stand device.

4.1.2 Biomechanics

In order to develop a wearable robot to perform the sit-to-stand motion, it is crucial to understand the biomechanics behind it. The robot must mimic the human knee and hip joint so that the motion could be repeated without discomfort or pain to the user. Sitting-to-standing is one of the most complex tasks in daily living, as it requires large muscle forces and precise shifting of the body's Center of Mass (COM) [108]. On average, this motion takes about 1.8 seconds to complete, and during this motion the COM moves from low but fully supported position to an upright and stable standing position (Figure 4.2) [109, 110]. To start the motion, the trunk moves forward and hips flex, then as the weight shifts forward and lift off from the chair is achieved, the hips and knees extend until the standing position is reached. Sit-to-stand can be divided into four stages: weight shift, seat off, extension, and stabilization. The weight

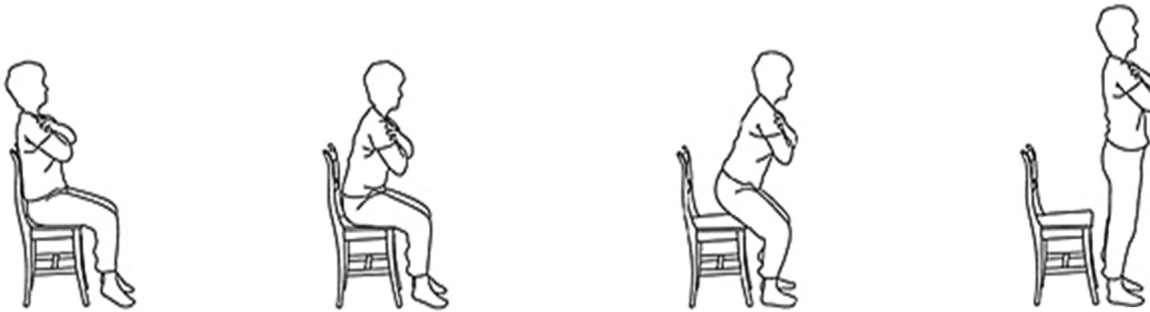


Figure 4.2: Sit-to-stand motion

shift phase takes up approximately 40% of the movement, and is the initialization of the motion [109]. During this phase the body's COM is displaced horizontally toward the feet [110]. To do so, the torso moves toward the knee, changing the hip angle from 80 degrees to 48 degrees [109]. While the hip is flexing, the knee is extending from 94 degrees to 106 degrees [109]. The seat off phase begins when the buttocks lifts off the chair, causing the body to be in a statically unstable position [108]. The COM is located posterior to the heel and outside of the

base of support, making it the most likely point of falling during the motion [108]. However, with enough horizontal momentum, sit-to-stand can be completed [108]. After seat off, the hips and knees extend throughout the rest of the motion. The hips extend from 48 degrees to 92 degrees, and the knees continue to extend from 106 degrees to 177 degrees when an upright standing position is reached [109]. As the body rises into a standing position, the COM shifts vertically and the body becomes more stable [110]. The rising portion of the motion accounts for approximately 60% of the movement, and requires the most muscle force [109]. The torque during the initial extension of the knee can be as high as 165 Nm for a 75 kg subject, which occurs when it is approximately 90 degrees [111]. The knees and hip extend at a constant velocity of 60 degrees/second during this time until a standing position is reached [112]. Once fully upright, the stabilization phase occurs to make sure the body remains upright.

4.2 Methods

4.2.1 Center of Mass Calculations

The primary goal of the sit-to-stand motion is to shift the body's COM from a low, fully supported position to an upright, stable one [110]. However, during the movement the body is in an statically unstable position, largely due to the position of the COM [108]. Therefore, when developing a wearable robot it is important to accurately model how the COM changes over the full sit-to-stand motion in order to decrease the risk of falling.

The first step of locating the COM was to determine the mass of each of the segments of interest (torso, thigh, shank). The mass of each was found in terms of percentage of body weight to make the model more adaptable to various body weights. Body mass data was based on anthropometric studies conducted by Plagenhoef *et al.* and the Naval Biodynamics Laboratory, which have been used as standards for anthropometric measurements [113, 114]. Based on the Naval base research, the shank accounted for 6 percent of the body mass, the thigh for 12 percent, and the torso (and rest of the body) for the other 82 percent of the body mass [114]. Similarly, based on the studies conducted by Plagenhoef *et al.*, the shank accounted for 5 percent of the body mass, the thigh for 11 percent and the torso (and rest of the body) for the other 84 percent. For the simulation of the device, the body mass percentages from the Naval Biodynamics Laboratory were used.

Then, the position of the COM in each of the segments had to be found before calculating the overall COM. The location of the COM of each segment was also found in terms of percentages to make the model more adaptable. For both the shank and thigh segments, the COM was located at 43 percent of the total length (measured from the distal end of the bone), and for the torso the COM was located at 50 percent of the total length (Figure 4.3) [113].

The average length of the shank and thigh were found to be 43.03 cm and 50.5 cm respectively, and these were the lengths used for the frame of the wheelchair [115]. However, due to the design of the proposed wheelchair device, the length of the torso segment had to be calculated and optimized to be as close to the anatomical length of the human torso as possible. The proposed wheelchair device has back wheels that fold up into the backrest when standing up. Therefore the length of the torso had to match the length of the back leg of the device. To calculate the maximum length of the back leg, the device was considered to be on a 15 degree ramp with the ankle, knee, and hip all at right angles. A 15 degree ramp was chosen based on the regulation for the maximum angle a wheelchair ramp can be (7 degrees) with a safety factor of two [116, 117].

In Figure 4.4, the ramp angle (θ) was considered to be 15 degrees, meaning the resting back leg angle (ϕ) had to be less than or equal to 75 degrees. The goal was for the back leg length (l) to be as close to the average human torso length as possible, while still being able to support the frame. The relationship between the back leg length and the resting back leg angle is shown (4.1):

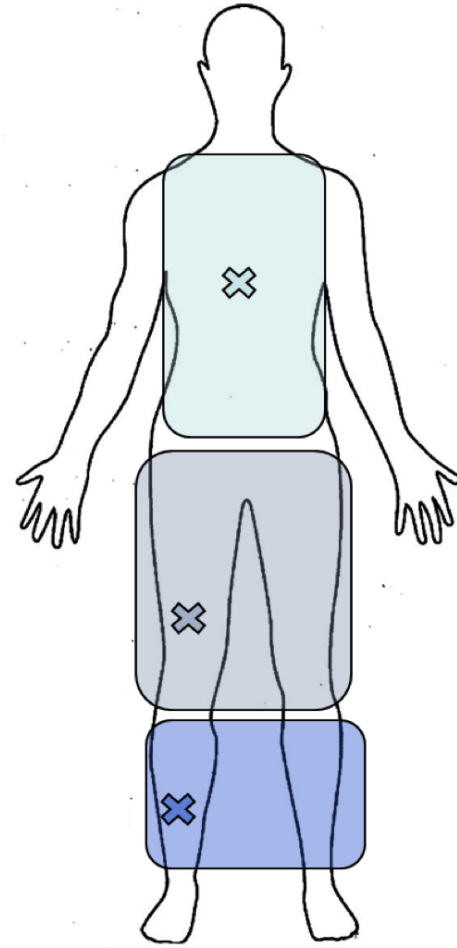


Figure 4.3: The approximate locations of the center of mass of each of the segments of interest

$$l = 43\text{cm}/\sin\theta \quad (4.1)$$

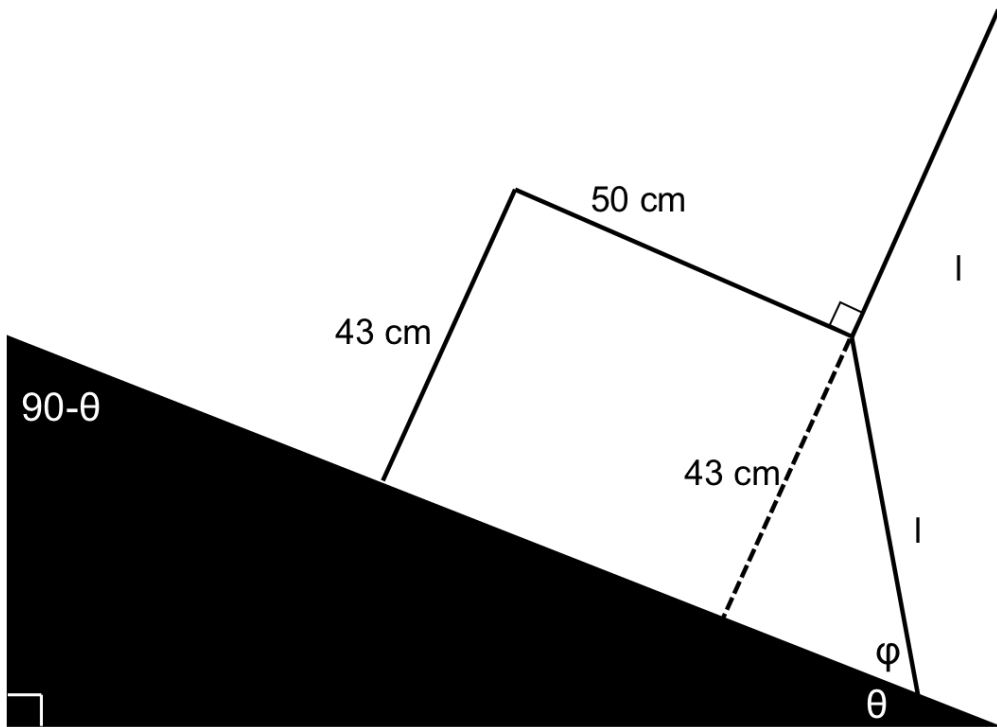
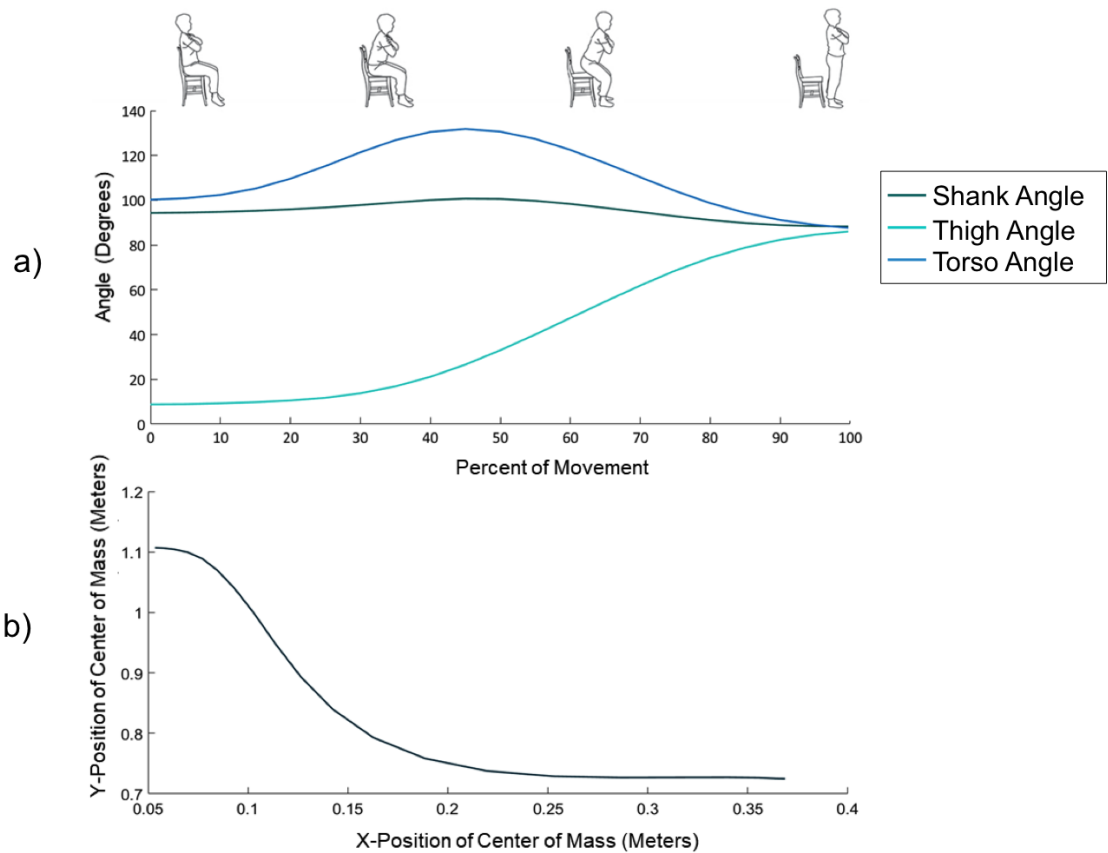


Figure 4.4: Free body diagram for determining the length of the back wheel for a 15 degree ramp

The resting angle was constrained to be less than or equal to 75 degrees because the sum of the ramp angle and the resting back leg angle had to be less than or equal to 90 degrees. It was found that when $\phi = 47$ degrees, the back leg length was 58.4 cm, which is equal to the average length of the human torso [114]. Based on these calculations, the length of the back wheel and therefore torso was chosen to be 58.4 cm. After these variables were found, the change in COM of each segment as well as the overall change in COM of a 90 kg person performing sit-to-stand was calculated and plotted (Figure 4.5).

4.2.2 Component Selection

The next stage of designing the assistive sit-to-stand device was to decide on the component to use in order to raise the user into a standing position. For the proposed design to be able to support a 90 kg person while sitting and throughout the entire sit-to-stand motion, the proper components need to be chosen. These components should closely mimic the anthropometric



- a) Change in center of mass of each segment of interest during STS
- b) Overall change in center of mass during STS

Figure 4.5: Change in center of mass during sit-to-stand

measurements, and must be able to support the large joint forces experienced at the knee. Due to the knee requiring the most muscle force during the sit-to-stand motion, the knee was the focus of the design. The proposed knee design comprised of a linear actuator combined with a leaf-spring mechanism, which would mimic the knee's natural range of motion. For the device to be wearable, the frame had to match the length of the shank and thigh of an average person, matching the lengths used in the COM calculations. The location of the COM of the body was also used to calculate the amount of torque at the knee (Figure 4.6).

The upward force the linear actuator experiences had to match the torque about the knee in order to function as the knee joint in the proposed design. This was calculated by summing

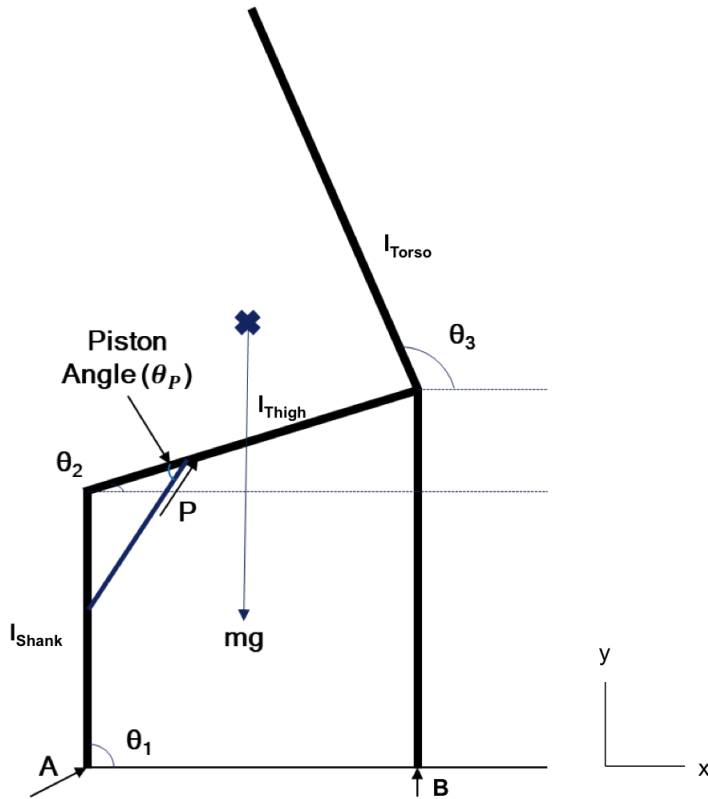


Figure 4.6: Free body diagram of the wheelchair frame used to calculate the force on the linear actuator

the forces in the y-direction multiplied by the perpendicular distance from the knee (4.2).

$$\Sigma\tau = (P\sin\theta_p * d_p) - (mg * com_x) + (B * d_t) + (A\cos\phi * d_s) \quad (4.2)$$

P was considered the force of the piston, which was the only unknown in this equation. Based on previous literature, the knee can experience upwards of 165 Nm of force during the sit-to-stand motion [111]. When scaled for a 90 kg person, the torque the knee experiences can reach 200 Nm. Therefore, the linear actuator had to be able to push with enough force to match the 200 Nm torque experienced about the knee. Based on (4.2), the linear actuator experienced approximately 200 N of force at rest, so the actuator had to be strong enough to support at least 200 N of force in addition having a long enough stroke length to fully extend the knee. This lead to the ECO-WORTHY Linear Actuator Motor DC 12V Heavy Duty 330lb 400MM

Stroke Length (DCHouse, United Kingdom) being chosen as the linear actuator to be used in the next stage of the design. After the necessary amount of force and torque was calculated, the optimal placement of the linear actuator on the frame had to be found. The ideal placement of the actuator would provide enough upwards force to raise the user without providing too much force on the shank. Too much force pushing against the shank would make the user's leg kick out, and cause them to fall. The constraints on the optimization were the maximum length of the piston (0.38 meters) and the amount of necessary force (200 Nm). From these constraints, the potential forces in both the normal and x-directions were calculated and plotted (4.3) (Figure 4.7). The optimal placement of the linear actuator was chosen to be 0.14 meters away from the knee, at a 54 degree angle (as shown by the blue box in Figure 4.7). This will allow for the full range of motion to be completed while also providing enough lifting support to complete the standing motion.

$$\tau = x * F_N \quad (a)$$

$$F_x = F_N / \tan\theta = 200/y \quad (b)$$

$$l_p = x^2 + y^2 \quad (c)$$

$$l_pMax = 0.38m$$

$$l_pMin = 0.26m$$

(4.3)

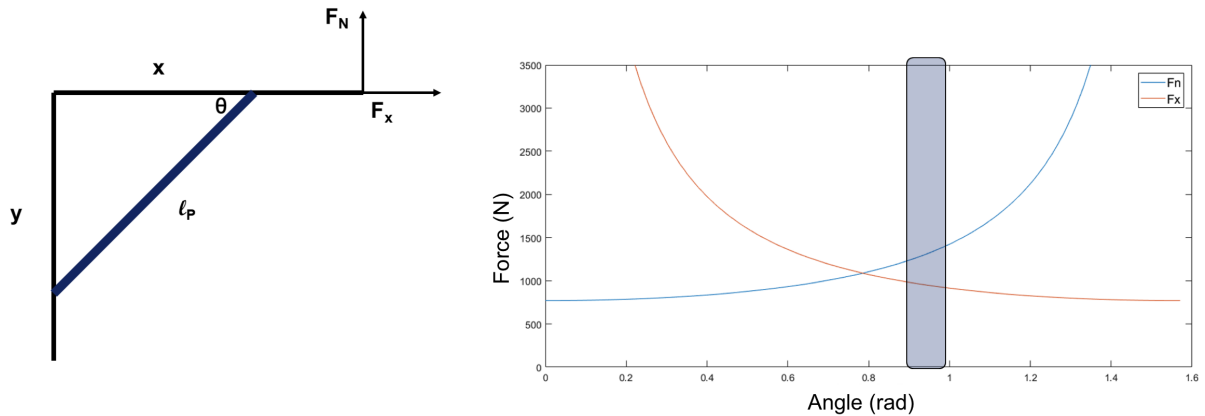


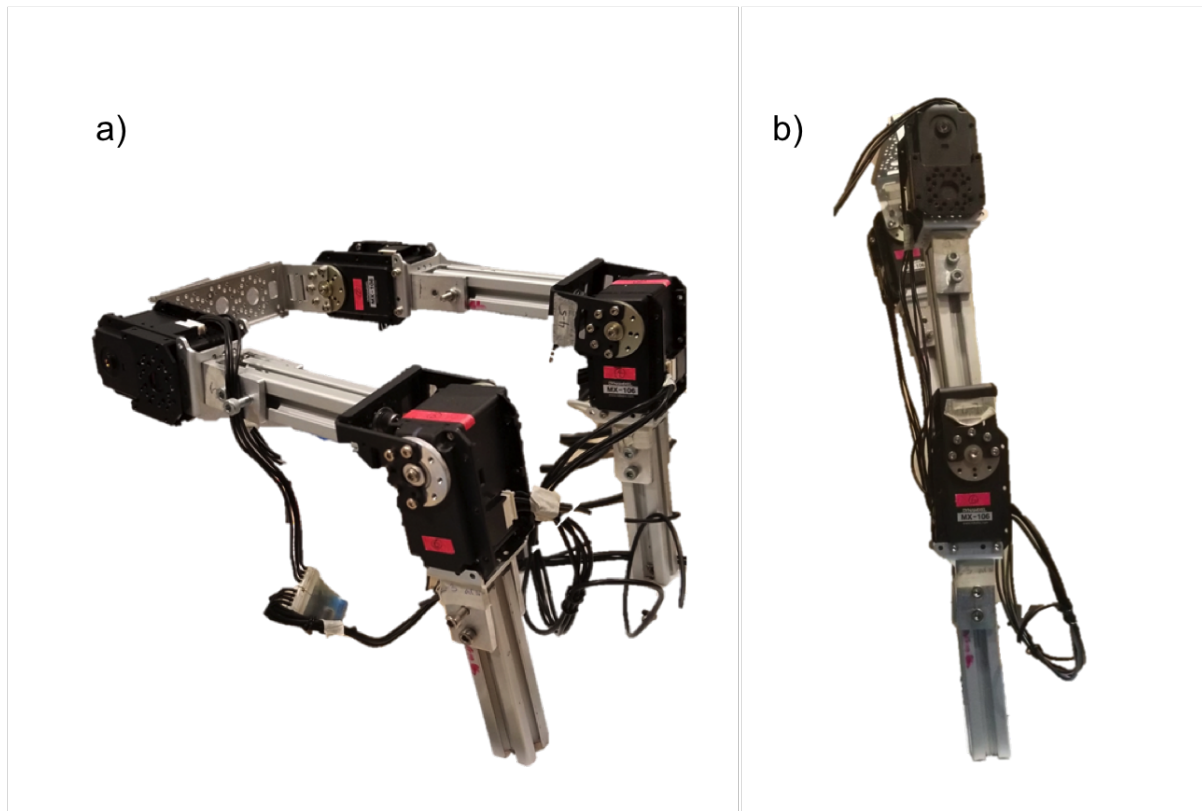
Figure 4.7: Optimization of the linear actuator placement

4.2.3 Scaled Down Model

To ensure the design was plausible, a scaled down table-top model that could complete the sit-to-stand motion had to be built. The first step in scaling down the model was to determine mathematically how the mass proportion changed. Solidworks was used test how the mass of the body and each of the segments changes for different scaling factors. The relationship for this scaling was found and used in the next stage of calculations. The next step in scaling the model was to scale the lengths of the limbs so that the torque produced was proportional to the 200 Nm of torque naturally experienced. The four Dynamixel Mx106 motors, which each generate 3.5 Nm of torque were used in this model, so the goal was to scale the length of the limbs down to produce this much torque. (4.3).

$$s^4 = \tau_{Knee} / \tau_{Dynamixel} \quad (4.3)$$

Based off the calculations, the lengths of the limb had to be scaled down by 2.75 in order to create an accurate table-top model. The results of this are shown in Figure 4.8.



a) Tabletop model of the wheelchair frame in sitting mode
b) Tabletop model of the wheelchair frame in standing mode

Figure 4.8: Tabletop model of the wheelchair frame

4.3 Discussion

A scaled down tabletop model of the proposed device that can complete the sit-to-stand motion was built. This model follows the biomechanics of the sit-to-stand motion as outlined by Nuzik *et al.*. The benefit to using the Dynamixel motors is that position and speed can be independently controlled in each of the four motors, so a variety of simulated scenarios can be tested. In addition, the motors can provide position feedback without additional equipment. This tabletop model only makes up part of the wheelchair, so future work will add on the two back wheels as well as a backrest. After the two back wheels are added, various retraction mechanisms can be tested to determine the optimal mechanism to use in the final product. One potential retraction mechanism is a fold-up mechanism, where the back wheels swing up and into the backrest of the wheelchair when standing mode is initiated. The wheels would first slide forward, helping to bend the torso and shift the COM forward, thus contributing to the first phase of the sit-to-stand motion. Then, as the body rises into a standing position, the wheels will fold up. This potential design is what the current model was based on, which is why the length of the torso segment was calculated. However, another potential mechanism to test could be a telescoping arm. This would allow the backrest of the seat to be shorter and potentially less cumbersome to the user. The telescoping arm may not be able to support the entire frame due to the higher probability of strain occurring in each joint of the arm. Other potential designs will also be simulated and tested. In addition to the retraction method for the back wheels, the placement and retraction method for the front wheels must be developed. One possibility is to develop a custom shoe that can house a retractable wheel. This shoe can also be modified for use with the ankle module since the ankle module is customized to the individual user. Either a spring or a solenoid could be used for this retraction mechanism.

The tabletop model is just the first step in developing a novel wheelchair that can transform into a gait assistive exoskeleton. The wheelchair will be comprised of modules that when put together make up both the chair and the exoskeleton. The low-cost assistive ankle device described in Chapter 3 of this paper will make up an optional add-on module for the wheelchair. A novel knee design for a sit-to-stand assistive device will be another module of the wheelchair. As previously mentioned, the proposed idea for the novel assistive knee module is a leaf spring mechanism combined with a linear actuator. One end of the leaf spring will be fixed while the other will be passively controlled by a spring so the center of the arc will match the changing knee angle. This design will actively assist the knee with extension through the linear actuator while following its natural range of motion by use of the leaf springs. Combining the leaf spring mechanism with a linear actuator is a novel method for performing knee extension and flexion, and could overcome the limitation of rigid exoskeletons which can impede the natural movement of the knee. The leaf spring design will also take advantage of the frame of the wheelchair so that the minimal amount of extra weight and components will be added. While this design idea has potential, other ideas for the novel knee design will be tested in order to determine the optimal design that works the best in the wheelchair framework.

After the knee module and the retraction mechanism is designed, the next step is to create a hip module that can target both flexion/ extension of the hip in addition to abduction and adduction of the hip. This hip module will be responsible for not only rotating the backrest of the wheelchair during the sit-to-stand movement, but for actuating the hip joints during walking. Therefore, these hip joints must have the functionality to perform two different modes. The sit-to-stand mode can be automated because it will follow the same trajectory each time it is activated. However, the walking mode should be more adaptable so that the user can operate the device in a variety of settings. The walking mode should also only assist as needed so that the

user is encouraged to perform as much of the movement they are capable of completing. Once the hip, knee, and ankle modules are completed, the next step is combining the three modules to create a full leg of an assistive wearable robot. Since most current wearable robots actively control the hip and knee joints while keeping the ankles passive, the ankle module can be an optional add-on module for the overall device. Depending on the user's needs, either one, two, or no ankle devices can be added to the knee and hip. If the ankle device is not added, then the ankles will be kept passive like in typical exoskeletons. The most crucial part of combining the three devices together will be the placement of the motors. For instance, the motor of the ankle device needs to be placed in precisely the right spot in order to continuously maintain tension on the cable while walking. In the current design as presented in Chapter 3, the motor was placed on the hip. This could overlap with the motors for hip flexion and extension. This problem should be kept in mind when designing each module, but will still need to be addressed when combining the three together into an assistive wearable robot. Another important aspect to consider is how the data from all three devices will be processed and controlled simultaneously. Once these challenges are addressed, the next step would be to modify the assistive wearable robot to become a transforming wheelchair. The wheels and wheel retraction mechanisms would have to be added on, as would a seat between the two leg frames. The seat should be soft and flexible, allowing the person to walk without restriction. Armrests could also be added to the completed device to ensure the arms stay in a steady and stable position during sit-to-stand. This would ensure the COM trajectory stays closer to the modelled one and decrease the variability during repetitions of the motion. The armrests could also provide an ideal place to house a remote controller or joystick to control both the wheelchair and the exoskeleton. The tabletop model presented in this chapter can be used to test these ideas to determine which is the best to use in the proposed transforming wheelchair device.

Chapter 5

Conclusions

The aim of this paper is to address the current limitations in wearable robotics by presenting a novel low-cost soft assistive device for ankle dorsi- and plantarflexion as well as the preliminary designs for a standing wheelchair with a novel knee joint. While more work still needs to be conducted before the device can be tested clinically, a prototype of a low-cost soft device for drop-foot was developed. This device can move the foot into position for both heel-strike and toe-off based on real time classification of stage of gait. Currently, the speed of the dorsi- or plantarflexion movement is based on the changing angle of the foot. Besides making the system wireless, the main step before the device can be tested clinically is developing a more robust control system. Once the control system is refined, the device should be tested clinically to ensure the functionality of the system. Accurately designing the 3D-printed shoe insole will be an important factor to consider before testing the ankle device on multiple people. Currently, the 3D-printed shoe insole is designed to replace the user's shoe insole, and the toe sensor is placed based on the location of the ball of the foot. This placement may have to vary depending on the user's foot, otherwise inaccurate force measurements from the toe sensor will be recorded. Inaccurate readings from the force sensors could detrimentally impact the control system by causing a wrong classification from the gaussian naive bayes classifier that was used in the system. However, this is a relatively simple problem to overcome since the force sensors are not embedded into the shoe insole. They can easily be moved to the correct position at the ball of the foot. The adaptability of the system to the individual is the main advantage of this ankle device over current rigid exoskeletons. Due to the minimalist approach of using as

few sensors and motors as possible, the developed ankle device is less expensive than typical exoskeletons. Another advantage is that unlike currently used AFOs, the developed ankle device does not restrict the ankle. This promotes moving the ankle as much as possible, which is healthier for the user unlike traditional AFOs which promote a pattern of nonuse. Even with the current limitations, the developed low-cost soft wearable ankle device showed potential for use as an assistive walking device.

The final result of the preliminary design for a standing wheelchair was a tabletop model of the system. This model was anatomically accurate, and was able to precisely follow the sit-to-stand motion. The model will allow for testing of other components of the full design, such as the retractable back wheels, without needing to build them to scale initially. The motors used in the tabletop model can easily be controlled to follow different trajectories at various speeds. This feature will be useful in simulating the full design before building it to scale. In addition to simulating the standing wheelchair, future work will use the ideas presented to develop a novel knee design to be integrated into the wheelchair frame. In the future, these two devices could be combined to form a novel device that can assist with both walking and sit-to-stand.

Bibliography

- [1] Lisa I. Iezzoni, Ellen P. McCarthy, Roger B. Davis, and Hilary Siebens. Mobility difficulties are not only a problem of old age. *Journal of General Internal Medicine*, 16(4):235–243, 2001.
- [2] S. Mefoued, S. Mohammed, Y. Amirat, and G. Fried. Sit-to-Stand movement assistance using an actuated knee joint orthosis. *Proceedings of the IEEE RAS and EMBS International Conference on Biomedical Robotics and Biomechatronics*, pages 1753–1758, 2012.
- [3] Joel Stein, Lauri Bishop, Daniel J. Stein, and Christopher Kevin Wong. Gait training with a robotic leg brace after stroke: A randomized controlled pilot study. *American Journal of Physical Medicine and Rehabilitation*, 93(11):987–994, 2014.
- [4] Amira Boukadida, France Piotte, Patrick Dehail, and Sylvie Nadeau. Determinants of sit-to-stand tasks in individuals with hemiparesis post stroke: A review. *Annals of Physical and Rehabilitation Medicine*, 58(3):167–172, 2015.
- [5] Angel Gil-Agudo, Marta Solís-Mozos, Antonio J. Del-Ama, Beatriz Crespo-Ruiz, Ana Isabel De La Peña-González, and Soraya Pérez-Nombela. Comparative ergonomic assessment of manual wheelchairs by paraplegic users. *Disability and Rehabilitation: Assistive Technology*, 8(4):305–313, 2013.
- [6] Yosuke Eguchi, Hideki Kadone, and Kenji Suzuki. Standing mobility vehicle with passive exoskeleton assisting voluntary postural changes. *IEEE International Conference on Intelligent Robots and Systems*, pages 1190–1195, 2013.

- [7] Giulio Rosati. The place of robotics in post-stroke rehabilitation. *Expert Review of Medical Devices*, 7(6):753–758, 2010.
- [8] Anindo Roy, Hermano I. Krebs, Shawnna L. Patterson, Timothy N. Judkins, Ira Khanna, Larry W. Forrester, Richard M. Macko, and Neville Hogan. Measurement of Human Ankle Stiffness Using the Anklebot. *2007 IEEE 10th International Conference on Rehabilitation Robotics, ICORR’07*, 00(c):356–363, 2007.
- [9] Melissa Morris. A Review of Rehabilitation Strategies for Stroke Recovery. *ASME Early Career Technical Conference*, 11(October):24–31, 2015.
- [10] Wenda C Carlyle, James B Mcclain, Abraham R Tzafriri, Lynn Bailey, G Brett, Peter M Markham, James R L Stanley, Elazer R Edelman, Concord Biomedical Sciences, Emerging Technologies, and Lexington Technology Park. HHS Public Access. 162(3):561–567, 2015.
- [11] S. Tasseel-Ponche, A. P. Yelnik, and I. V. Bonan. Motor strategies of postural control after hemispheric stroke. *Neurophysiologie Clinique*, 45(4-5):327–333, 2015.
- [12] Slavka Viteckova, Patrik Kutilek, and Marcel Jirina. Wearable lower limb robotics: A review. *Biocybernetics and Biomedical Engineering*, 33(2):96–105, 2013.
- [13] 2015-foot-drop.
- [14] Ling Fung Yeung, Corinna Ockenfeld, Man Kit Pang, Hon Wah Wai, Oi Yan Soo, Sheung Wai Li, and Kai Yu Tong. Design of an exoskeleton ankle robot for robot-assisted gait training of stroke patients. *IEEE International Conference on Rehabilitation Robotics*, pages 211–215, 2017.

- [15] Mehol D. Patel, K. Tilling, E. Lawrence, A. G. Rudd, C. D.A. Wolfe, and C. McKevitt. Relationships between long-term stroke disability, handicap and health-related quality of life. *Age and Ageing*, 35(3):273–279, 2006.
- [16] A Bruno-Petrina. Motor Recovery In Stroke: Recovery Considerations, Theories of Recovery, Mechanisms of Recovery, 2016.
- [17] American Heart Association. Post-Stroke Rehabilitation, 2016.
- [18] Atsushi Tsukahara, Ryota Kawanishi, Yasuhisa Hasegawa, and Yoshiyuki Sankai. Sit-to-stand and stand-to-sit transfer support for complete paraplegic patients with robot suit HAL. *Advanced Robotics*, 24(11):1615–1638, 2010.
- [19] Renée M. Hakim, Brandon G. Tunis, and Michael D. Ross. Rehabilitation robotics for the upper extremity: review with new directions for orthopaedic disorders. *Disability and Rehabilitation: Assistive Technology*, 12(8):765–771, 2017.
- [20] Bing Chen, Hao Ma, Lai Yin Qin, Fei Gao, Kai Ming Chan, Sheung Wai Law, Ling Qin, and Wei Hsin Liao. Recent developments and challenges of lower extremity exoskeletons. *Journal of Orthopaedic Translation*, 5:26–37, 2016.
- [21] Peter S. Lum, Charles G. Burgar, Peggy C. Shor, Matra Majmundar, and Machiel Van der Loos. Robot-assisted movement training compared with conventional therapy techniques for the rehabilitation of upper-limb motor function after stroke. *Archives of Physical Medicine and Rehabilitation*, 83(7):952–959, 2002.
- [22] Hermano I. Krebs, Laura Dipietro, Shelly Levy-Tzedek, Susan E. Fasoli, Avrielle Rykman-Berland, Johanna Zipse, Jennifer A. Fawcett, Joel Stein, Howard Poizner, Al-

- bert C. Lo, Bruce T. Volpe, and Neville Hogan. A paradigm shift for rehabilitation robotics. *IEEE Engineering in Medicine and Biology Magazine*, 27(4):61–70, 2008.
- [23] Ho Shing Lo and Sheng Quan Xie. Exoskeleton robots for upper-limb rehabilitation: State of the art and future prospects. *Medical Engineering and Physics*, 34(3):261–268, 2012.
- [24] Paweł Maciejasz, Jörg Eschweiler, Kurt Gerlach-hahn, Arne Jansen-troy, and Steffen Leonhardt. Open Access A survey on robotic devices for upper limb rehabilitation. pages 1–29, 2014.
- [25] Radiology Management, ICU Management, Healthcare IT, Cardiology Management, Executive Management.
- [26] Ing Lucia Koukolová. OVERVIEW OF THE ROBOTIC REHABILITATION SYSTEMS FOR UPPER LIMB REHABILITATION. Technical report.
- [27] Anindo Roy, Larry W. Forrester, Richard F. Macko, and Hermano I. Krebs. Changes in passive ankle stiffness and its effects on gait function in people with chronic stroke. *The Journal of Rehabilitation Research and Development*, 50(4):555, 2013.
- [28] R. A.R.C. Gopura, D. S.V. Bandara, Kazuo Kiguchi, and G. K.I. Mann. Developments in hardware systems of active upper-limb exoskeleton robots: A review. *Robotics and Autonomous Systems*, 75:203–220, 2016.
- [29] Yong Lae Park, Jobim Santos, Kevin G. Galloway, Eugene C. Goldfield, and Robert J. Wood. A soft wearable robotic device for active knee motions using flat pneumatic artificial muscles. *Proceedings - IEEE International Conference on Robotics and Automation*, pages 4805–4810, 2014.

- [30] Hong Kai Yap, James Cho, Hong Goh, Raye Chen, and Hua Yeow. 6th European Conference of the International Federation for Medical and Biological Engineering. 45:367–370, 2015.
- [31] Ashley M. Stewart, Christopher G. Pretty, Mark Adams, and Xiao Qi Chen. Review of Upper Limb Hybrid Exoskeletons. *IFAC-PapersOnLine*, 50(1):15169–15178, 2017.
- [32] G Colombo, M Joerg, R Schreier, and V Dietz. Treadmill training of paraplegic patients using a robotic orthosis. *Journal of rehabilitation research and development*, 37(6):693–700, 2000.
- [33] Jan F. Veneman, Rik Kruidhof, Edsko E.G. Hekman, Ralf Ekkelenkamp, Edwin H.F. Van Asseldonk, and Herman Van Der Kooij. Design and evaluation of the LOPES exoskeleton robot for interactive gait rehabilitation. *IEEE Transactions on Neural Systems and Rehabilitation Engineering*, 15(1):379–386, 2007.
- [34] Alberto Esquenazi, Mukul Talaty, and Arun Jayaraman. Powered Exoskeletons for Walking Assistance in Persons with Central Nervous System Injuries: A Narrative Review. *PM and R*, 9(1):46–62, 2017.
- [35] Katherine A. Strausser and H. Kazerooni. The development and testing of a human machine interface for a mobile medical exoskeleton. *2011 IEEE/RSJ International Conference on Intelligent Robots and Systems*, pages 4911–4916, 2011.
- [36] Adam B Zoss, Homayoon Kazerooni, and Andrew Chu. Biomechanical Design of the Berkeley Lower Extremity Exoskeleton (BLEEX). *IEEE/ASME Transactions on Mechatronics*, 11(2):128–138, 2006.
- [37] Conference Paper and Yoshiyuki Sankai. Robotics Research. 70(January 2007), 2011.

- [38] Zhiyong Yang, Yuguang Zhu, Xiuxia Yang, and Yuanshan Zhang. Impedance control of exoskeleton suit based on RBF adaptive network. *2009 International Conference on Intelligent Human-Machine Systems and Cybernetics, IHMSC 2009*, 1:182–187, 2009.
- [39] Peter D. Neuhaus, Jerryll H. Noorden, Travis J. Craig, Tecalote Torres, Justin Kirschbaum, and Jerry E. Pratt. Design and evaluation of Mina: A robotic orthosis for paraplegics. *IEEE International Conference on Rehabilitation Robotics*, 2011.
- [40] Letian Wang, Shiqian Wang, Edwin H.F. Van Asseldonk, and Herman Van Der Kooij. Actively controlled lateral gait assistance in a lower limb exoskeleton. *IEEE International Conference on Intelligent Robots and Systems*, pages 965–970, 2013.
- [41] Simone Marcheschi, Fabio Salsedo, Marco Fontana, and Massimo Bergamasco. Body extender: Whole body exoskeleton for human power augmentation. *Proceedings - IEEE International Conference on Robotics and Automation*, pages 611–616, 2011.
- [42] Nevio Luigi Tagliamonte, Fabrizio Sergi, Giorgio Carpino, Dino Accoto, and Eugenio Guglielmelli. Human-robot interaction tests on a novel robot for gait assistance. *IEEE International Conference on Rehabilitation Robotics*, 1, 2013.
- [43] CONOR JAMES WALSH, KEN ENDO, and HUGH HERR. a Quasi-Passive Leg Exoskeleton for Load-Carrying Augmentation. *International Journal of Humanoid Robotics*, 04(03):487–506, 2007.
- [44] H. He and K. Kiguchi. A study on EMG-based control of exoskeleton robots for human lower-limb motion assist. *Proceedings of the IEEE/EMBS Region 8 International Conference on Information Technology Applications in Biomedicine, ITAB*, 00:292–295, 2008.

- [45] Rocco Salvatore Calabrò, Alberto Cacciola, Francesco Bertè, Alfredo Manuli, Antonino Leo, Alessia Bramanti, Antonino Naro, Demetrio Milardi, and Placido Bramanti. Robotic gait rehabilitation and substitution devices in neurological disorders: where are we now? *Neurological Sciences*, 37(4):503–514, 2016.
- [46] Tingfang Yan, Marco Cempini, Calogero Maria Oddo, and Nicola Vitiello. Review of assistive strategies in powered lower-limb orthoses and exoskeletons. *Robotics and Autonomous Systems*, 64:120–136, 2015.
- [47] Allan Joshua Veale and Shane Quan Xie. Towards compliant and wearable robotic orthoses: A review of current and emerging actuator technologies. *Medical Engineering and Physics*, 38(4):317–325, 2016.
- [48] REX Bionics.
- [49] Indego, 0.
- [50] Cyberdyne. What’s HAL.
- [51] Inho Kim, Woonghee Cho, Gyunghwan Yuk, Hyunseok Yang, Byeong Rim Jo, and Byung Hoon Min. Kinematic analysis of sit-to-stand assistive device for the elderly and disabled. *IEEE International Conference on Rehabilitation Robotics*, 2011.
- [52] Aaron M. Dollar and Hugh Herr. Lower Extremity Exoskeletons and Active Orthoses: Challenges and State-of-the-Art. *IEEE Transactions on Robotics*, 24(1):144–158, 2008.
- [53] ReWalkTM Personal 6.0 - ReWalk – More Than Walking.
- [54] The world’s first cyborg-type robot - Cyberdyne Hal robotic exoskeleton to help paralyzed - Photos: Cyberdyne Hal robotic exoskeleton to... | TECHNO TEC | Pinte....

- [55] Ekso GT - Exoskeleton Report.
- [56] ihmc Robotics.
- [57] National Institute of Neurological Disorders and Stroke. Foot Drop Information Page.
- [58] Ira Khanna, Anindo Roy, Mary M. Rodgers, Hermano I. Krebs, Richard M. MacKo, and Larry W. Forrester. Effects of unilateral robotic limb loading on gait characteristics in subjects with chronic stroke. *Journal of NeuroEngineering and Rehabilitation*, 7(1):1–8, 2010.
- [59] JW Pritchett, MA Porembski, and VK. Panchbhavi. Foot Drop: Background, Anatomy, Pathophysiology.
- [60] Hisashi Naito, Yasushi Akazawa, Kensuke Tagaya, Takeshi Matsumoto, and Masao Tanaka. An ankle-foot orthosis with a variable-resistance ankle joint using a magnetorheological-fluid rotary damper. *Journal of Biomechanical Science and Engineering*, 4(2):182–191, 2009.
- [61] Wolfgang Svensson and Ulf Holmberg. Ankle-foot-orthosis control in inclinations and stairs. *2008 IEEE International Conference on Robotics, Automation and Mechatronics, RAM 2008*, 00:301–306, 2008.
- [62] Arkady Polinkovsky, Richard J. Bachmann, Nicole I. Kern, and Roger D. Quinn. An Ankle Foot Orthosis with insertion point eccentricity control. *IEEE International Conference on Intelligent Robots and Systems*, pages 1603–1608, 2012.
- [63] Gregory S. Sawicki and Nabil S. Khan. A Simple Model to Estimate Plantarflexor Muscle-Tendon Mechanics and Energetics During Walking With Elastic Ankle Exoskeletons. *IEEE Transactions on Biomedical Engineering*, 63(5):914–923, 2016.

- [64] Seyoung Kim, Youngsu Son, Sangkyu Choi, Sangyong Ham, and Cheolhoon Park. Design of a simple, lightweight, passive-elastic ankle exoskeleton supporting ankle joint stiffness. *Review of Scientific Instruments*, 86(9), 2015.
- [65] Thomas Seel, Cordula Werner, and Thomas Schauer. The adaptive drop foot stimulator – Multivariable learning control of foot pitch and roll motion in paretic gait. *Medical Engineering and Physics*, 38(11):1205–1213, 2016.
- [66] J Blaya and H Herr. Adaptive Control of a Variable-Impedance Ankle-Foot Orthosis to Assist Drop Foot Gait. *Neural Systems and Rehabilitation Engineering, IEEE Transactions on*, 12(1):24–31, 2004.
- [67] Hiroshi Takemura, Takayuki Onodera, Ding Ming, and Hiroshi Mizoguchi. Design and control of a wearable stewart platform-type ankle-foot assistive device. *International Journal of Advanced Robotic Systems*, 9:1–7, 2012.
- [68] Michael D. Castro. Ankle biomechanics. *Foot and ankle clinics*, 7(4):679–693, 2002.
- [69] Moroz A. Physical Therapy (PT) - Special Subjects.
- [70] Harrison P Crowell Iii and Angela C Boynton. Crowell III 2002 - Exoskeleton Power and Torque Requirements Based on Human Biomechanics.pdf. (November), 2002.
- [71] C. R. Ethier and Craig a. Simmons. *Introductory Biomechanics From Cells to Organisms*. 2007.
- [72] Chaitanya Nutakki, Jyothisree Narayanan, Aswathy Anitha Anchuthengil, Bipin Nair, and Shyam Diwakar. Classifying gait features for stance and swing using machine learning. *2017 International Conference on Advances in Computing, Communications and Informatics, ICACCI 2017*, 2017-Janua:545–548, 2017.

- [73] Jason Brownlee. Naive Bayes for Machine Learning, 2016.
- [74] Mathworks. Applying Supervised Learning.
- [75] Stanford University. The Bernoulli Model.
- [76] Niklas Donges. The Logistic Regression Algorithm, 2018.
- [77] Jason Brownlee. Logistic Regression for Machine Learning, 2016.
- [78] Linear SVC Machine Learning SVM example with Python.
- [79] Scikit-learn Developers. `sklearn.multiclass.OneVsRestClassifier`, 2017.
- [80] One-vs-All Classification, 2013.
- [81] IITK Robotics Club. Introduction to PID Control.
- [82] Katja Mombaur and Khai Long Ho Hoang. How to best support sit to stand transfers of geriatric patients: Motion optimization under external forces for the design of physical assistive devices. *Journal of Biomechanics*, 58:131–138, 2017.
- [83] B. Allouche, A. Dequidt, L. Vermeiren, and P. Hamon. Design and control of a sit-to-stand assistive device via EtherCAT fieldbus. *Proceedings of the IEEE International Conference on Industrial Technology*, pages 761–766, 2017.
- [84] Joshua G. Vose, Arlene McCarthy, Eduardo Taccol, and Robert W. Horst. Optimization of lower extremity kinetics during transfers using a wearable, portable robotic lower extremity orthosis: A case study. *Biosystems and Biorobotics*, 1:99–102, 2013.
- [85] Philippa M. Dall and Andrew Kerr. Frequency of the sit to stand task: An observational study of free-living adults. *Applied Ergonomics*, 41(1):58–61, 2010.

- [86] Abul Doulah, Xiangrong Shen, and Edward Sazonov. A method for early detection of the initiation of sit-to-stand posture transitions. *Physiological Measurement*, 37(4):515–529, 2016.
- [87] PT in Motion. Report Predicts Coming PT, PTA Shortage in US, 2014.
- [88] Jaimie F. Borisoff, Johanne Mattie, and Vince Rafer. Concept proposal for a detachable exoskeleton-wheelchair to improve mobility and health. *IEEE International Conference on Rehabilitation Robotics*, 2013.
- [89] S Arthanat and W Strobel. Wheelchair ergonomics: implications for vocational participation. *Journal of Vocational Rehabilitation*, 24(2):97–109, 2006.
- [90] Renaldo Herdiano Putra, Ahmad Ghifari Wildan Rahman, Endah Suryawati Ningrum, and Didik Setyo Purnomo. Design and stress analysis on electric standing wheelchair. *Proceedings IES-ETA 2017 - International Electronics Symposium on Engineering Technology and Applications*, 2017-Decem:112–117, 2017.
- [91] Products | Products | English.
- [92] Eric Nickel, Andrew Hansen, Jonathan Pearlman, and Gary Goldish. A drive system to add standing mobility to a manual standing wheelchair. *Assistive Technology*, 28(4):218–224, 2016.
- [93] Sunrise Medical Quickie Jive Up Powerchair.
- [94] Standing Wheelchairs, Upright Wheelchair & Mobility Products, UK, Shropshire | Genie Wheelchairs.
- [95] Stand Up Wheelchairs - Standing Wheelchair XO Series.

- [96] Toyota iBOT Motorized Wheelchair Design and Specs.
- [97] Elevation by PDG - The Elevation supports increased function, independence, and comfort.
- [98] Manual Standing Wheelchair | Shirley Ryan AbilityLab - Formerly RIC.
- [99] Up n Go | Easy-Walking.
- [100] laddroller.
- [101] Takuya Furusawa, Takayuki Sawada, Nobuaki Fujiki, Ryoichi Suzuki, and Eberhard P. Hofer. Practical assistive device for sit-to-stand tasks. *2017 IEEE 6th Global Conference on Consumer Electronics, GCCE 2017*, 2017-Janua(Gcce):1–3, 2017.
- [102] Omar Salah, Ahmed Asker, Ahmed M R Fath El-Bab, Samy M F Assal, Ahmed A Ramadan, Salvatore Sessa, and Ahmed Abo-Ismail. Development of parallel manipulator sit to stand assistive device for elderly people. *2013 Ieee Workshop on Advanced Robotics and Its Social Impacts (Arso)*, pages 27–32, 2013.
- [103] Bingquan Shen, Jinfu Li, Fengjun Bai, and Chee-Meng Chew. Development and control of a lower extremity assistive device (LEAD) for gait rehabilitation. *2013 IEEE 13th International Conference on Rehabilitation Robotics (ICORR)*, pages 1–6, 2013.
- [104] Roman Kamnik and Tadej Bajd. Human voluntary activity integration in the control of a standing-up rehabilitation robot: A simulation study. *Medical Engineering and Physics*, 29(9):1019–1029, 2007.
- [105] Daisuke Chugo, Wataru Matsuoka, Songmin Jia, and Kunikatsu Takase. Rehabilitation walker system for standing-up motion. *IEEE International Conference on Intelligent Robots and Systems*, pages 3367–3372, 2007.

- [106] Alter G: Bionic Leg Research.
- [107] Peter Paul Pott, Sebastian Immanuel Wolf, Julia Block, Stefan Van Drongelen, Markus Grün, Daniel W.W. Heitzmann, Jürgen Hielscher, Andreas Horn, Roman Müller, Oliver Rettig, Ulrich Konigorski, Roland Werthschützky, Helmut Friedrich Schlaak, and Thorsten Meiß. Knee-ankle-foot orthosis with powered knee for support in the elderly. *Proceedings of the Institution of Mechanical Engineers, Part H: Journal of Engineering in Medicine*, 231(8):715–727, 2017.
- [108] Masahiro Fujimoto and Li Shan Chou. Dynamic balance control during sit-to-stand movement: An examination with the center of mass acceleration. *Journal of Biomechanics*, 45(3):543–548, 2012.
- [109] S. Nuzik, R. Lamb, A. VanSant, and S. Hirt. Sit-to-stand movement pattern. A kinematic study. *Physical Therapy*, 66(11):1708–1713, 1986.
- [110] W. Mathiyakom, J. L. McNitt-Gray, P. Requejo, and K. Costa. Modifying center of mass trajectory during sit-to-stand tasks redistributes the mechanical demand across the lower extremity joints. *Clinical Biomechanics*, 20(1):105–111, 2005.
- [111] DEVELOPMENT OF ROBOTIC LOWER-LIMB PROSTHETIC AND ORTHOTIC DEVICES by SAROJ THAPA XIANGRONG SHEN , COMMITTEE CHAIR HWAN-SIK YOON Submitted in partial fulfillment of the requirements for the degree of Master of Science in the Department of Mechanical Engine. 2015.
- [112] Kenton R. Kaufman, Kai Nan An, and Edmund Y.S. Chao. A comparison of intersegmental joint dynamics to isokinetic dynamometer measurements. *Journal of Biomechanics*, 28(10), 1995.

- [113] S Plagenhoef. Anatomical Data for Analyzing Human Motion. *Research Quarterly for Exercise and Sport*, 54, 1983.
- [114] J Haley and J Haley. Anthropometry and Mass Distribution for Human Analogues. *Aamrl-Tr-88-010*, (March), 1988.
- [115] Top 10 Longest Bones in the Human Body, 2014.
- [116] Northeast Rehabilitation Health Network. Wheelchair Ramp Information, 2018.
- [117] Wheelchair Ramps Guidelines and Best Practice, 2017.